

Project No. 09-765

# ALD Coatings on $Gd_2O_3$ Burnable Poison Nanoparticles and Carbonaceous TRISO Coating Layers

---

Reactor Concepts RD&D

Dr. Alan Weimer

University of Colorado, Boulder

Douglas Marshall, Technical POC

Madeline Feltus, Federal POC

## Final Report

**Project Title:** ALD Coatings on Gd<sub>2</sub>O<sub>3</sub> Burnable Poison Nanoparticles and Carbonaceous TRISO Coating Layers

**Covering Period:** October 1, 2009 to September 30, 2012

**Date of Report:** November 8, 2012

**Recipient:** University of Colorado  
3415 Colorado Avenue  
JSCBB Campus Box 596 UCB  
Boulder, CO 80309-0596

**Award Number:** Contract 00090607

**Project Number:** 09-765

**Principal Investigator:** Alan W. Weimer, Department of Chemical and Biological Engineering, University of Colorado, Boulder, CO 80303-0596;  
[alan.weimer@colorado.edu](mailto:alan.weimer@colorado.edu)

## **Project Objective**

The objective of this project was to demonstrate the feasibility of using atomic layer deposition (ALD) to apply ultrathin neutron-absorbing, corrosion-resistant layers consisting of ceramics, metals, or combinations thereof, on particles for enhanced NNGP fuel pellets. The manufactured composite particles will ideally be used to address materials issues with Generation IV nuclear power plants, using scaled-up powder coating techniques developed at the University of Colorado.

This project was divided into two specific aims, one to address the primary degradation mechanism of the fuel pellet core, and one to address the primary degradation mechanism of the protective shells of the fuel pellet. The success of either of these concepts will lead to significant advancement toward solving materials issues in NNGP fuel pellets.

## Background

The proposed project scope falls under two main specific aims: 1) fabrication and analysis of Gd-containing ceramics via gas-phase functionalization of  $Gd_2O_3$  powders with ceramic coatings; 2) coating and analysis of graphite/carbide powders with the chemically inert  $ZrO_2/Zr_3N_4$ -containing layers on outer surfaces and within pores for carbon-based fuel pellet shell strengthening. The activities contained within this project are designed to improve the lifetime of NGNP fuel pellets

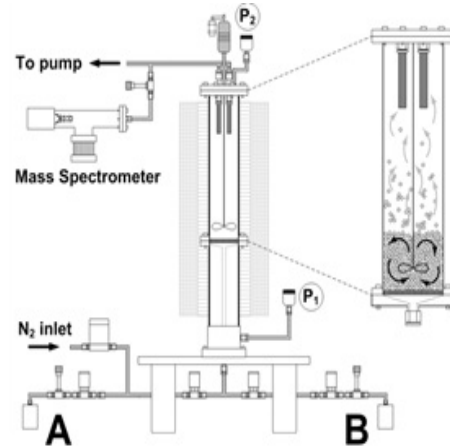


Figure 1. Schematic of ALD fluidized bed reactor.

Each of these specific aims can be achieved using the ALD technique, which has been used to deposit ceramic, metal and hybrid ceramic/polymer films on a variety of nano- and micron-sized particle (and other high surface area) substrates. Metal oxides and nitrides deposit in the form of conformal, pinhole-free films of nanoscale thickness, and metals tend to deposit as dispersed islands, resulting in nanoclusters of atoms. Experimental design techniques, either a factor analysis (full or fractional) or a central composite design (CCD) will be employed for the completion of each Milestone, as appropriate.

ALD is an analog of chemical vapor deposition (CVD) where reactive vapor precursors are administered to a reactor system individually, which chemically bonds one monolayer of the precursor (the “A” half-reaction) with all surface functional groups under saturating exposures. Upon completion, the first reactant is purged from the system, and the second one is then administered into the reactor, effectively eliminating an opportunity for gas-phase side-reactions. The second reaction, or “B” half-reaction, is allowed to proceed to completion before the B precursor is purged from the system. The sequential administration (or “dosing”) of each precursor can build a wide variety of ceramic films with angstrom-level precision. A schematic of the fluidized bed reactor used for Particle ALD is shown in Figure 1. ALD is an analog of CVD, but the two techniques are viable over two vastly different process windows. ALD is designed for ultrathin, precision-thickness films, whereas CVD is more ideal for building thick films where precision, conformity or porosity-free properties are not as critical. The process windows are shown in Figure 2.

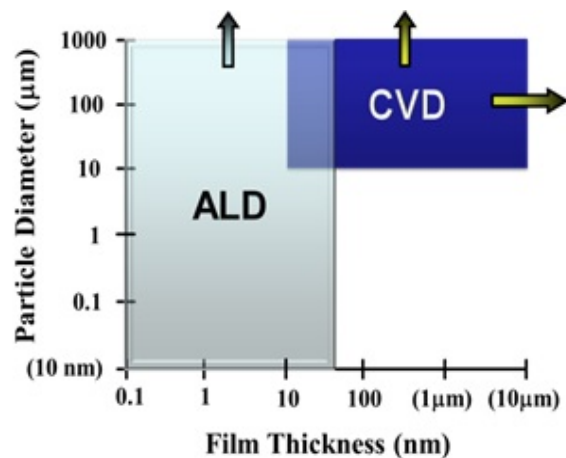


Figure 2. ALD and CVD process windows.

## Specific Aim 1 Outline

### *Improvements to the Fuel Pellet Core*

From a survey of recent literature, the composition and method of producing the NGNP fuel pellet kernel is a solid state reaction between primarily  $\text{UO}_2$  and  $\text{Gd}_2\text{O}_3$  powders. Current research efforts include evaluating additives, typically ceramics, which can be incorporated during the solid state reaction with the goal of improving the thermomechanical properties of the composite core. From a design perspective, the roles of the uranium-containing and gadolinium-containing components of the kernel are known as the source and moderator of neutron fluency, respectively.

The design goals of Specific Aim 1:

- a) **Improve structural integrity** of  $\text{Gd}_2\text{O}_3$  through incorporation of ceramic sub-phases without sacrificing too much gadolinium. The increasing content of a ceramic sub-phase is expected to increase structural integrity, while the decreasing content of the  $\text{Gd}_2\text{O}_3$  phase is expected to decrease neutron moderation capabilities. As such there is expected to be an optimal content ratio where value is added as measured by an improved fuel kernel lifetime.
- b) **Quantify thermal properties** of composite powders for modeling purposes. The predicted lifetime of the composite system should be modeled in order to optimize the content between the  $\text{Gd}_2\text{O}_3$  phase and the ceramic sub-phase. It is also thought that the energy required to form a mixed-metal oxide using solid state sintering techniques will be lower when using ALD-coated powders relative to the blending and sintering of primary oxide powders due to the lack of interdiffusion required for the former composition. An understanding of the energy requirements to manufacture the particles will help model the production cost at any scale.
- c) **Quantify crystal structure** and other physical properties of the produced ceramic composite powders. Both the content and crystal structure of the gadolinium oxide phase are important, as the thermomechanical properties of monoclinic  $\text{Gd}_2\text{O}_3$  has yielded a longer lifetime throughout its neutron absorption lifetime than the cubic phase. In addition, it is unknown precisely how the formation of mixed-metal oxides (e.g.  $\text{GdAlO}_3$ ,  $\text{Gd}_2\text{TiO}_4$ , etc.) will behave when derived using the atomic layer deposition process to produce the ceramic sub-phase. The grain size of a system typically has direct implications on its mechanical properties, with smaller grains leading to a decreased likelihood of crack propagation. Therefore the crystal structure, composition and grain size of each structure are important for predicting the expected gains in NGNP kernel technology using the ALD technique.
- d) **Quantify mechanical properties** of Gd-containing ceramic matrix composites, including thermal expansion. One failure mode for NGNP fuel pellets is the migration of the kernel in the direction of least resistance. Any anisotropy to

thermal flux and/or thermal expansion coefficients will increase the probability of catastrophic failure of the system. Sound methods should be devised and followed to demonstrate the tensile strength of the composite system.

## Specific Aim 1 Results

First, the cost of various  $Gd_2O_3$  sources were investigated as well as some of the particle characteristics that affect performance as an ALD substrate and neutron absorption material, such as BET Surface Area and crystal structure, respectively. The cost of micron-sized  $Gd_2O_3$  particles was found to be equivalent to the cost of gadolinium oxalate hydrate particles, on a per-Gd basis.  $Gd_2O_3$  nanopowder approaches four times the cost of other  $Gd_2O_3$  substrates. The surface area of  $Gd_2O_3$  derived through the decomposition of the gadolinium oxalate powder had eight times the surface area of the micron-sized  $Gd_2O_3$  powder. Incorporation of ceramic phases by ALD surface coatings is more efficient on a higher surface area powder (process time to achieve target weight percent) so gadolinium oxalate as the source material is favorable. Cryogenic milling of the gadolinium oxalate powder did not yield a dramatic increase in surface area (via particle size reduction), so the process intensity of the milling process is not worth the cost. Industrially produced  $Gd_2O_3$  nanopowder has the highest surface area but is unjustifiably expensive when compared to the performance of the  $Gd_2O_3$  powder derived from Gd-oxalate decomposition.

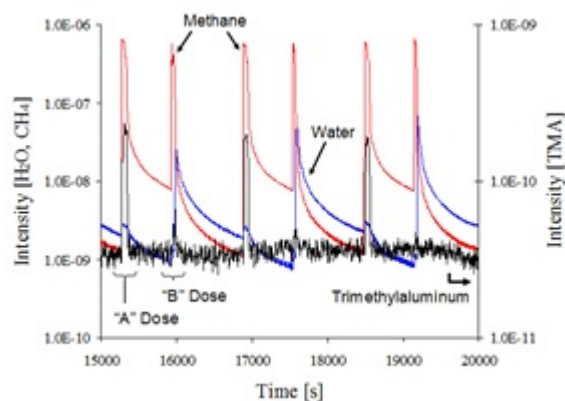


**Figure 3. Mass spectrometry data for three arbitrary consecutive  $Al_2O_3$  ALD cycles coated on  $Gd_2O_3$  particles. TMA, water, and their reaction product, methane, are shown.**

The incorporation of  $Al_2O_3$  phases onto  $Gd_2O_3$  powders using the ALD technique was successful. A typical mass spectrometry plot is shown in Figure 3, which tracks the evolution of methane throughout an  $Al_2O_3$  reaction process between trimethylaluminum (TMA) and water. TEM images were taken for the composite powders with the highest alumina contents, and are shown in Figure 4. The conformal, nano-scale films can be seen very clearly for all samples. The high quality results observed were of typical precision for Particle ALD.

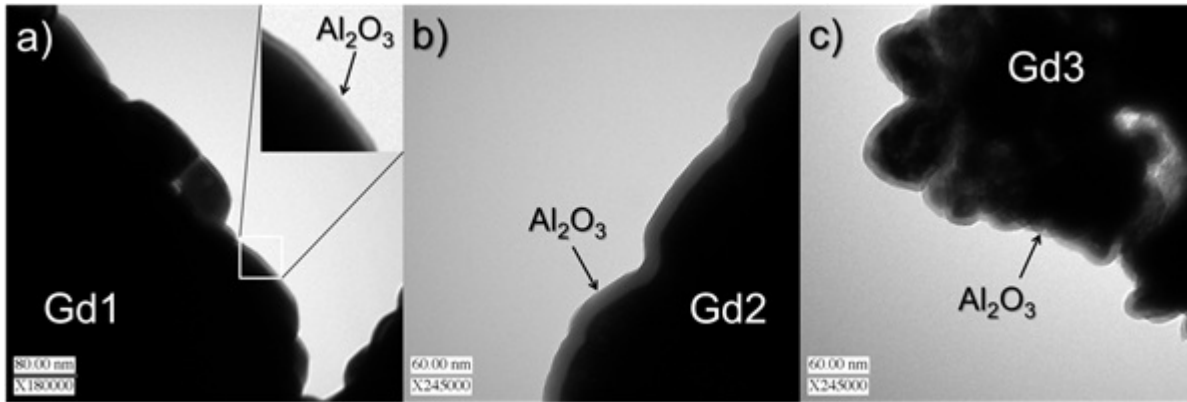


Figure 4. TEM images of Al<sub>2</sub>O<sub>3</sub> ALD films deposited on Gd<sub>2</sub>O<sub>3</sub> particles: (a) 100 cycles; (b) 60 cycles; (c) 40 cycle.

Attempts were also made to deposit films other than alumina, namely TiO<sub>2</sub> and Gd/Gd<sub>2</sub>O<sub>3</sub>. The difficulties associated with TiO<sub>2</sub> ALD proved to be insurmountable, and using the typical, inexpensive TiO<sub>2</sub> precursors, TiCl<sub>4</sub> and H<sub>2</sub>O, was detrimental to the particle substrate. TiO<sub>2</sub> via TiCl<sub>4</sub> converted the surface of the Gd<sub>2</sub>O<sub>3</sub> powder into GdCl<sub>3</sub>, which was highly undesirable so the task was abandoned. A Gd<sub>2</sub>O<sub>3</sub> ALD process was also attempted, and though the deposition reactions were successful, it was determined that the low growth rate and relatively high cost of the precursor made it an imprudent strategy, especially in light of the very positive results of the Al<sub>2</sub>O<sub>3</sub> ALD process on Gd<sub>2</sub>O<sub>3</sub> substrates.

Initially, compact fabrication techniques were developed to form stable pellets via cold pressing followed by sintering at atmospheric pressure. The thermal expansion of the uncoated Gd<sub>2</sub>O<sub>3</sub> blended with alumina nanopowder, as well as the alumina-coated gadolinia was measured using the dilatometer procured through a NEUP Infrastructure award. The thermal expansion of ALD-coated powders was found to be generally lower than the expansion of pellets that consist of blended powders. This is attributed to the homogeneous coating process, which guarantees that the alumina content is identical on both a macroscopic and microscopic level.

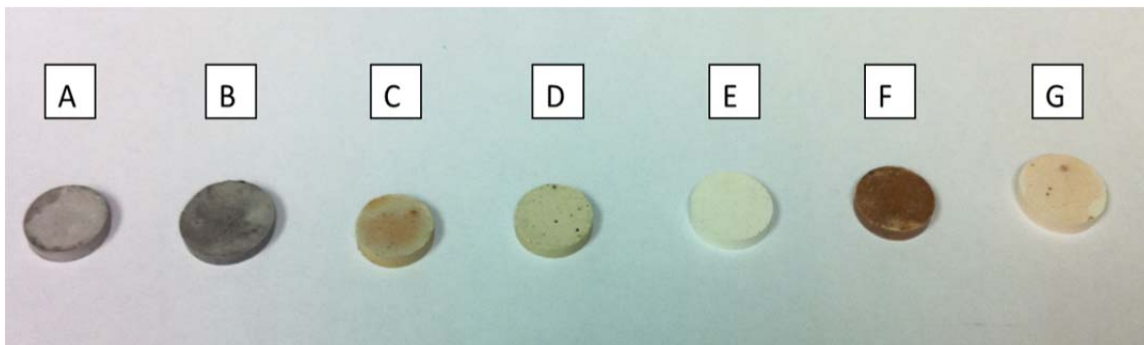


Figure 5. Photograph of coated and uncoated gadolinium (III) oxide pellets cold-pressed and sintered to 1450°C in air. (A) Gd<sub>2</sub>O<sub>3</sub> from Gd-Ox, (B) Gd<sub>2</sub>O<sub>3</sub> from Sigma Aldrich, (C) 9 Al<sub>2</sub>O<sub>3</sub> on Gd<sub>2</sub>O<sub>3</sub> from cryomilled Gd-Ox Decomp, (D) 20 Al<sub>2</sub>O<sub>3</sub> on Gd<sub>2</sub>O<sub>3</sub> from cryomilled Gd-Ox, (E) 12 Al<sub>2</sub>O<sub>3</sub> on Gd<sub>2</sub>O<sub>3</sub> from Gd-Ox Decomp, (F) 40 Al<sub>2</sub>O<sub>3</sub> on Gd<sub>2</sub>O<sub>3</sub> from Gd-Ox Decomp, (G) 60 Al<sub>2</sub>O<sub>3</sub> on Gd<sub>2</sub>O<sub>3</sub> from Gd-Ox Decomp.

The dilatometer results of these sintered pellets are presented in Figure 6. The temperature range 300°C – 1100°C was used to calculate the coefficient of linear thermal expansion,  $\alpha_L$ . The tests were run at 1 K/min from 25°C to 1500°C in an argon atmosphere. CTE values from Figure 6. Strain data from 300C to 1100C. The slope of

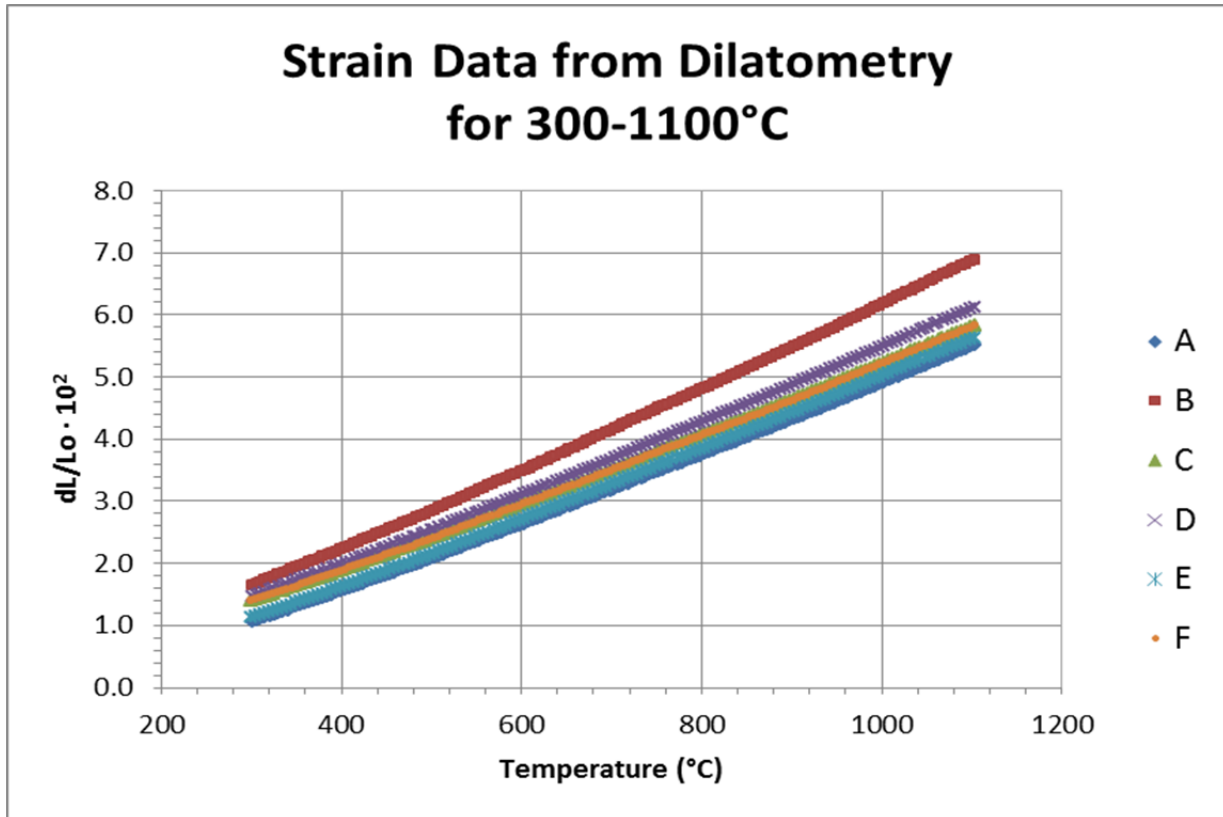


Figure 6. Strain data from 300C to 1100C. The slope of the line yields the coefficient of thermal expansion. (A) Uncoated Gd<sub>2</sub>O<sub>3</sub> from decomposed Gd-oxalate, (B) Uncoated Gd<sub>2</sub>O<sub>3</sub> from Sigma Aldrich, (C) 9 cycles ALD-Al<sub>2</sub>O<sub>3</sub> on Gd<sub>2</sub>O<sub>3</sub> from cryomilled-decomposed Gd-oxalate, (D) 20 cycles ALD-Al<sub>2</sub>O<sub>3</sub> Gd<sub>2</sub>O<sub>3</sub> from cryomilled-decomposed Gd-oxalate, (E) 12 cycles ALD-Al<sub>2</sub>O<sub>3</sub> on Gd<sub>2</sub>O<sub>3</sub> from decomposed Gd-oxalate, (F) 40 cycles ALD-Al<sub>2</sub>O<sub>3</sub> on Gd<sub>2</sub>O<sub>3</sub> from decomposed Gd-oxalate.

the line yields the coefficient of thermal expansion. (A) Uncoated Gd<sub>2</sub>O<sub>3</sub> from decomposed Gd-oxalate, (B) Uncoated Gd<sub>2</sub>O<sub>3</sub> from Sigma Aldrich, (C) 9 cycles ALD-Al<sub>2</sub>O<sub>3</sub> on Gd<sub>2</sub>O<sub>3</sub> from cryomilled-decomposed Gd-oxalate, (D) 20 cycles ALD-Al<sub>2</sub>O<sub>3</sub> Gd<sub>2</sub>O<sub>3</sub> from cryomilled-decomposed Gd-oxalate, (E) 12 cycles ALD-Al<sub>2</sub>O<sub>3</sub> on Gd<sub>2</sub>O<sub>3</sub> from decomposed Gd-oxalate, (F) 40 cycles ALD-Al<sub>2</sub>O<sub>3</sub> on Gd<sub>2</sub>O<sub>3</sub> from decomposed Gd-oxalate. are presented in Table 1.

Table 1. Calculated coefficients of linear thermal expansion for gadolinium (III) oxide sintered pellets.

	Uncoated Gd <sub>2</sub> O <sub>3</sub>		ALD-coated, Cryomilled Gd <sub>2</sub> O <sub>3</sub>		ALD-coated Gd <sub>2</sub> O <sub>3</sub> from decomp. Gd-ox	
	Gd <sub>2</sub> O <sub>3</sub> from Gd-ox	Sigma Aldrich Gd <sub>2</sub> O <sub>3</sub>	9 cyc. Al <sub>2</sub> O <sub>3</sub>	20 cyc. Al <sub>2</sub> O <sub>3</sub>	12 cyc. Al <sub>2</sub> O <sub>3</sub>	40 cyc. Al <sub>2</sub> O <sub>3</sub>

$\alpha_{L,300-1100C}$ [ $10^{-6}/K$ ]	53.7	62.7	53.4	55.3	54.3	53.3
---	------	------	------	------	------	------

From the data shown in Table 1, there is no clear relationship between ALD film thickness and linear coefficient of thermal expansion though from literature, a negative correlation was expected. It is evident that  $Gd_2O_3$  derived from the decomposition of Gd-oxalate has a reduced thermal expansion compared to industrially manufactured 99.9% pure gadolinium oxide powder.

Using a HIP after cold-pressing pellets maintained the shape of the compacts and was a viable route to producing reliable substrates. For additional rigidity before putting pellets into the HIP, a sintering step at atmospheric pressure also appears to be beneficial, if transporting materials between pieces of equipment is an issue during manufacturing. Interestingly, there was a color change between the starting powder and the sintered compacts believed to result from complete decomposition of the Gd-oxalate into  $Gd_2O_3$ .

An important component of thermo mechanical testing of the ALD-coated  $Gd_2O_3$  material was nano-indentation analysis to determine modulus of elasticity and hardness. These pellets were prepared by first cold-pressure compaction, followed by hot isostatic pressing to 1450°C and 100 MPa, and finally by polishing the test surface to 3 microns.

**Table 2. Nano-indentation results for  $Gd_2O_3$  substrates, some of which were coated with  $Al_2O_3$ -ALD.**

Sample Name	Avg. Modulus (GPa)	Std. Dev.	Avg. Hardness (GPa)	Std. Dev.	Avg. Unload Modulus (GPa)	Std. Dev.	Avg. Unload Hardness (GPa)	Std. Dev.
Commercial $Gd_2O_3$	81.6	31.9	2.95	1.91	72.8	22.5	2.86	1.41
25 $Al_2O_3$ on commercial $Gd_2O_3$	78.4	32.5	3.68	1.48	67.5	36.9	3.28	1.48
50 $Al_2O_3$ on commercial $Gd_2O_3$	72.9	28.1	2.66	1.93	71.8	20.0	2.55	1.26
$Gd_2O_3$ from cryomilled and decomposed Gd-oxalate	101	28.1	3.99	1.57	88.1	34.0	3.41	1.60
9 $Al_2O_3$ on $Gd_2O_3$ from cryomilled and decomposed Gd-oxalate	167	30.0	8.86	2.56	139	32.9	7.35	1.48
12 $Al_2O_3$ on $Gd_2O_3$ from cryomilled and decomposed Gd-oxalate	113	28.6	5.18	2.28	96.8	18.0	4.09	1.35
20 $Al_2O_3$ on $Gd_2O_3$ from decomposed Gd-oxalate	71.4	34.4	4.33	1.34	57.9	32.0	3.32	1.27

40 Al <sub>2</sub> O <sub>3</sub> on Gd <sub>2</sub> O <sub>3</sub> from decomposed Gd-oxalate	108	43.1	4.13	2.29	79.0	31.6	3.28	1.71
60 Al <sub>2</sub> O <sub>3</sub> on Gd <sub>2</sub> O <sub>3</sub> from decomposed Gd-oxalate	104	36.1	4.01	1.64	87.1	31.2	3.16	1.29

With respect to modulus of elasticity, there is a loose negative correlation to ALD film thickness. As the film thickness increases, the modulus of elasticity decreases, which is likely due the non-crystalline, amorphous structure of the ALD film. Unfortunately, no statistically significant assertion can be made with respect to ALD film thicknesses effect on elasticity and hardness due to the large standard deviation associated with each nano-indentation measurement presented in Table 2.

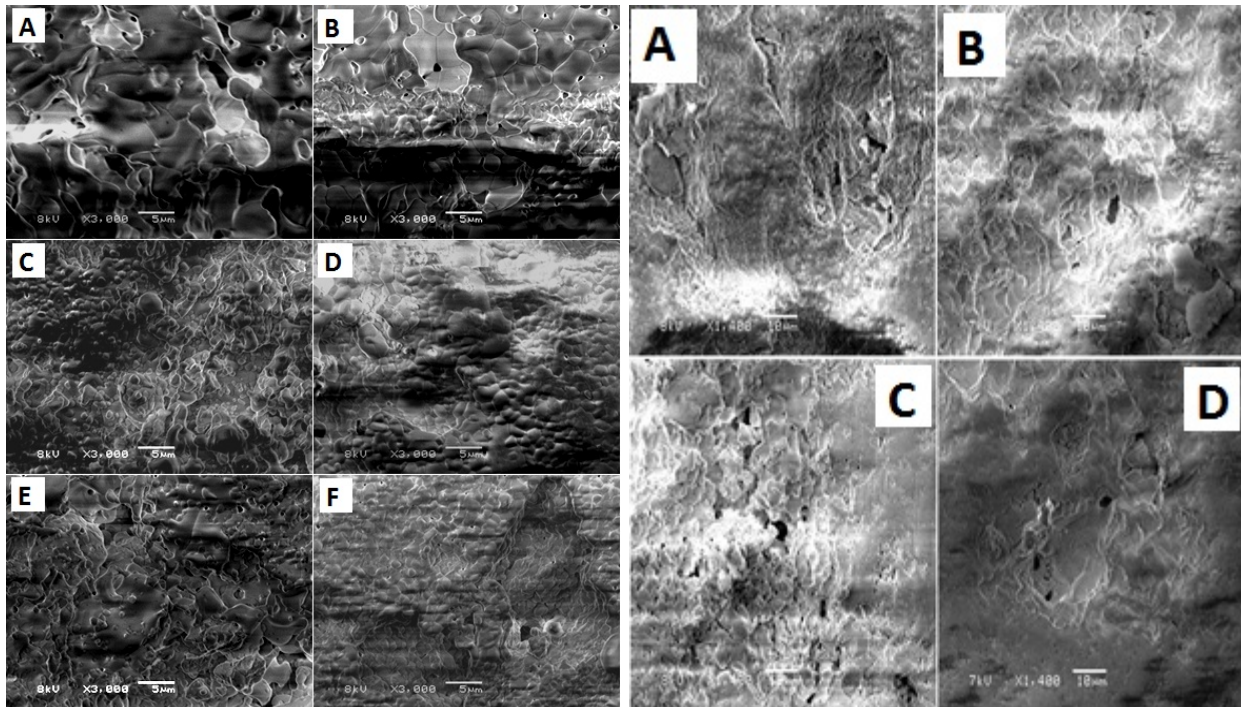


**Figure 7.** 3000X SEM images of sintered gadolinium oxide substrates and ALD-coated surfaces. (A) Uncoated Gd<sub>2</sub>O<sub>3</sub> from Gd-ox, polished gadolinium oxide pellets. (B) Uncoated Sigma Aldrich Gd<sub>2</sub>O<sub>3</sub>, (C) 9 cycles Gd<sub>2</sub>O<sub>3</sub> from Sigma-Aldrich, (D) 20 cycles Al<sub>2</sub>O<sub>3</sub> on Gd<sub>2</sub>O<sub>3</sub> from Gd-ox, (E) 12 cycles Al<sub>2</sub>O<sub>3</sub> on cryomilled Gd<sub>2</sub>O<sub>3</sub> from Gd-ox, (F) 40 cycles Al<sub>2</sub>O<sub>3</sub> on Gd<sub>2</sub>O<sub>3</sub> from Gd-ox.  
**Figure 8.** 1400X SEM images of sintered, HIPped, and uncoated substrates. (A) Uncoated Gd<sub>2</sub>O<sub>3</sub> from Gd-ox, polished gadolinium oxide pellets. (B) Uncoated Sigma Aldrich Gd<sub>2</sub>O<sub>3</sub>, (C) 9 cycles Gd<sub>2</sub>O<sub>3</sub> from Sigma-Aldrich, (D) 20 cycles Al<sub>2</sub>O<sub>3</sub> on Gd<sub>2</sub>O<sub>3</sub> from Gd-ox, (E) 12 cycles Al<sub>2</sub>O<sub>3</sub> on cryomilled Gd<sub>2</sub>O<sub>3</sub> from Gd-ox, (F) 40 cycles Al<sub>2</sub>O<sub>3</sub> on Gd<sub>2</sub>O<sub>3</sub> from Gd-ox.

The large standard deviations for each measurement (upwards of 50% of the mean value) were believed to be attributed to the amorphous structure of both the gadolinium substrates and the ALD films. Crystalline silica used to calibrate the nano-indentation instrument showed standard deviations of less than 5% for modulus of elasticity and hardness. High temperature and high pressure sintering performed in a hot isostatic press combined with surface polishing to 3 microns were intended to mitigate the large standard deviations but were unsuccessful. More reliable modulus of elasticity and hardness values could be obtained from crystalline composites, which might be achieved at temperatures approaching 1680°C.

Another important component of the thermochemical analysis of the  $Gd_2O_3$  material was SEM imagery to determine the grain size of the sintered gadolinia substrates. Figure 7 presents SEM images of sintered  $Gd_2O_3$  pellet surfaces and highlights the difference in grain size between coated and uncoated powders. Powders that were not coated with  $Al_2O_3$ -ALD show much larger grain size than those that were coated. Furthermore, powders coated with thicker  $Al_2O_3$  films showed smaller grain sizes after sintering than powders coated with thinner  $Al_2O_3$  films. Comparisons of similar substrates with either thin or thick coatings, C to E and D to F, respectively, show relationship between grain growth and ALD film thickness clear.

Figure 8 presents SEM photos obtained for fully dense pellets produced via cold-pressing followed by Hot Isostatic Pressing to 100 MPa and 1450°C that were polished to 3 microns on a diamond polishing wheel. It is evident from these images that the presence of  $Al_2O_3$  deposited via ALD simultaneously increases the uniformity of grain size and decreases the porosity, i.e. improves the sintering, for  $Gd_2O_3$ . ALD is demonstrated as a viable and effective method for increasing the final density of sintered substrates.

## Specific Aim 2

### *Improve the Lifetime of Carbonaceous TRISO Coating Layers*

The second specific aim was to coat nanometer-scale (or “nanothick”)  $ZrO_2$ , YSZ, BN/ $B_2O_3$  films on carbonaceous powders and test the high-temperature corrosion-resistance and thermo-mechanical properties of these chemically-inert ceramic materials. The CVD-derived, porous carbonaceous layers, namely C, PyC and SiC, are extremely sensitive to oxidation at high temperature, especially in low oxygen partial pressure environments found in nuclear reactors due to  $O_2$ , CO and  $H_2O$ . There is a desire to develop CVD techniques for ZrC as a method to provide enhanced corrosion-resistance to the fuel pellet layers. ALD techniques for  $ZrO_2$  and BN films have been demonstrated on particle surfaces, and YSZ and  $B_2O_3$  are simple extensions of proven technology. The ultimate goal is to deposit Zirconium-based coatings on carbonaceous substrates due to its low neutron absorption cross-section. Though BN may be very effective to create corrosion resistant carbons, it has the second highest neutron absorption cross section, making it a poor candidate for this aspect of the project. The precursor being used for Zr-based coatings is electronic grade tetrakis-(dimethylamido) Zirconium (TDMA-Zr), which is 99.99% pure. Hafnium absorbs neutrons at  $\sim 600x$  the rate of the equivalent amount of zirconium, and Hf is typically present in Zr compounds at 1-2%. The expense of this precursor is likely justified here, as the standard expense of removing Hf from Zr is alleviated through the purification of this compound.

Thus there was justification for this approach to providing corrosion-resistance properties to the porous CVD films due to the ability of ALD precursors to infiltrate pores and coat all exposed carbonaceous surfaces. Coated powders were tested using a high temperature thermogravimetric analyzer (HT-TGA) with dilute air environment in Argon.

The design goals of Specific Aim 2:

- a) **Develop ALD process methodologies to successfully coat carbons.** Carbonaceous materials are difficult to coat due to the lack of chemical functionality at the surfaces, and the ideal ALD technique relies on chemical bonding of molecular building blocks directly onto surfaces. There have been methods to physisorb molecules to the surfaces of carbons, and these and other molecules will be tested to obtain a pathway toward nano-functionalization.
- b) **Quantify high temperature oxidation resistance** of carbons after incorporation of ceramic sub-phases. Once the methodology has been developed,  $ZrO_2/Zr_3N_4$  and  $Y_2O_3/YN$  ALD processes can be developed and tested. It is thought that ceramic nitrides will have the greatest opportunity for success, as the presence of metal-nitrogen bonds tends to provide a much closer packed structure thus creating more effective diffusion barriers.
- c) **Quantify thermal cycling stability** of composite powders for modeling purposes. The thermal shock stability of ALD films will be a predictor of how well

the coatings will extend the lifetime of protective CVD layers on TRISO fuel pellets, and in turn provide a longer lasting nuclear fuel.

- d) **Identify potential fission byproduct scavenging materials.** This is an important goal that was not originally included in this proposal at the time it was written, and was added after attending the NEUP working meeting at ORNL in July 2010. Metals that can behave as either a cation or an anion have the greatest chance of being deposited by ALD (e.g. metal oxides or nitrides) and also be suitable for alloying to fission products and promote scavenging (e.g. silicides or aluminides). This is a strategy that deserves to be studied in Year 3 of this project, though may be difficult to validate experimentally without coating real, rather than surrogate, TRISO fuel pellets.

## Specific Aim 2 Results

As described in previous reports, coatings on carbons can be very difficult due to the inconsistent nature of surface functional groups. Methods to coat carbons must be developed case-to-case, as it is difficult to predict a carbonaceous substrate's functionality for ALD surface chemistry. Table 3 provides an overview of the historical progress made in the Weimer lab with using ALD to coat carbon particles, including work both within and outside the scope of this grant. The carbon substrate of most relevance to this project is the pyrolytic CVD carbon coated  $ZrO_2$  (TRISO surrogate) particles. Figure 9 shows TEM images along with corresponding EDS results of  $Al_2O_3$  and  $TiO_2$  ALD coatings successfully applied to carbon particles.

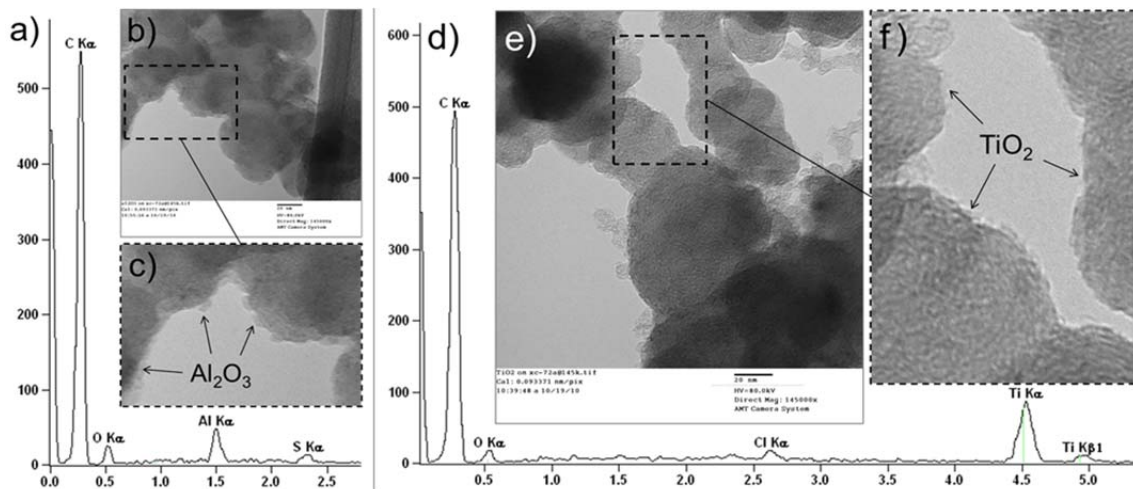


Figure 9. TEM images and EDS spectra of (a-c)  $Al_2O_3$  and (d-f)  $TiO_2$  on Cabot XC-72R carbon black.

Initially, the suitability of the TDMA-Zr precursor to  $ZrO_2$  ALD films for use in this project was determined by the following criteria: cost and ALD viability. Due to the low vapor pressure of TDMA-Zr at room temperature, heat was applied to the outer surface of the container to increase vapor pressure of the liquid inside. If future optimization is pursued, the center of the process window is 350°C. Though YSZ is a very good

candidate for a high strength coating material,  $ZrO_2$  has a very high thermal expansion coefficient, albeit decreasing with increasing  $Y_2O_3$  content. Therefore it may be beneficial to include  $Al_2O_3$ , or even high temperature metals such as Molybdenum or Tungsten, in multilayered fashion to the coating material of choice for cost reduction purposes while not sacrificing strength and oxidation resistance. The thermal expansion coefficients of many of the nitrides are about 50-60% of those of their oxides, and as such, the selection of each is transferrable across types of ceramics.

**Table 3. Description of relevant experience with performing ALD on carbonaceous substrates.**

Description	Coating Material(s)	Comments
Multi-walled carbon nanotubes	$Al_2O_3$	Conformal coating successful
Single-walled carbon nanotubes	$Al_2O_3$	Conformal coating unsuccessful; pre-treatment needed: $NO_2$ functionalization worked at small scale, liquid-phase pre-treatment (ethanol, surfactants) and drying prior to coating worked well
Diamond powder	$Al_2O_3$	Conformal coating successful
Graphite	$Al_2O_3$	Conformal coating unsuccessful; $NO_2$ functionalization did not work at larger scale
SPI Glassy Carbon	$Al_2O_3$	Conformal coating successful
Cabot XC-72R Vulcanized Carbon	$Al_2O_3$ , Alucone, $TiO_2$ , $B_2O_3$	Fuel Cell Grade Powder. Island growth successful, conformal coating limited by dispersion of sulfur sites from vulcanization process
TDA Research Carbon Black	$Al_2O_3$	Ultracapacitor Grade Powder. Difficult to coat, though surface area is $1900\text{ m}^2/\text{g}$ and may not be representative of difficult chemistry as much as non-ideal batch size
Pyrolytic CVD on surrogate TRISO	$Al_2O_3$ with surfactant pretreatment	Surfactant pretreatment process successfully led to ALD of alumina; 2Q11 focused on surfactant-free approaches

Initial laboratory efforts were focused around demonstration of ALD coatings on TRISO surrogate fuel pellets.  $Al_2O_3$  ALD from TMA and water by pre-treating the TRISO particles with sodium dodecylsulfate, a powerful surfactant was the first attempt. Figure 10 presents an SEM image of the coated TRIS particles with three locations where EDS mapping was performed: (1) the bulk surface, (2) within the bulk carbon layer of a cross-sectioned particle, and (3) the clearly white layer on the outer surface of the particle.

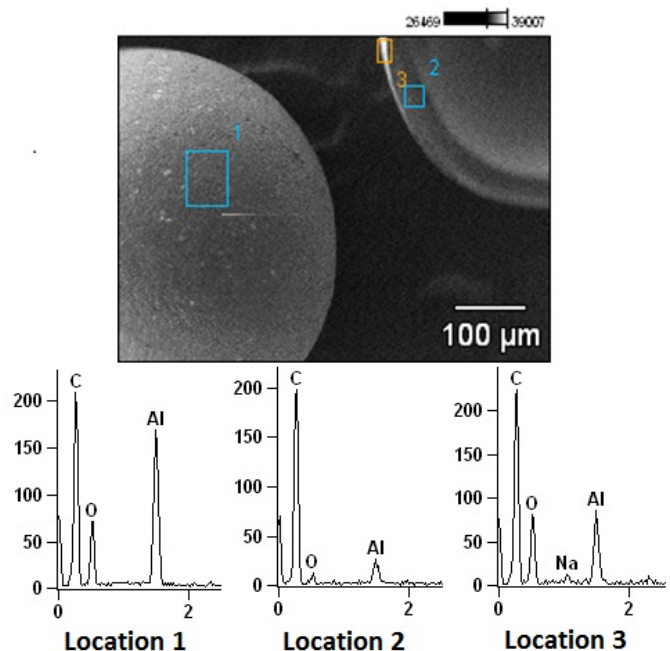


**Figure 10.** SEM and EDS mapping of TRISO surrogate fuel particles at three locations.

The surfactant pretreatment approach can be used to successfully deposit alumina on this type of carbon powder. As seen in the bulk surface spectrum (Location 1), the amount of surface aluminum is very close to the amount of carbon. The EDS spectrum of the carbon shell cross-section (Location 2) validates that the ALD process can infiltrate the porous CVD carbon network, though not as much as what can be coated on the external surface. This conclusion may be confounded by the liquid-phase surfactant pretreatment approach, as the liquid cannot penetrate through a porous layer as a gas-phase precursor can. From the cross-section of the outer edge of the carbon shell (Location 3) it is clear that some small amount of sodium remained on the TRISO pellet surface as a residual of the surfactant treatment. This is similar to what has been observed using this approach when coating single walled carbon nanotubes, and as such, was not surprising.

Subsequently, a surfactant-free ALD approach was developed for depositing  $\text{Al}_2\text{O}_3$  and  $\text{SiO}_2$  on to the pyrolytic carbon shell. Figure Image A shows SEM and EDS mapping spectra from an ALD process where we carried out a multilayered ALD process, where 5  $\text{Al}_2\text{O}_3$  and 5  $\text{SiO}_2$  cycles were deposited per layer, and 20 multilayers were deposited. Evidence that both alumina and silica were present was confirmed, as well as the presence of residual chlorine from the  $\text{SiCl}_4$  precursor.

It was found that the presence of chlorine could be greatly reduced by altering key process conditions. The EDS mapping spectra below are from a 40 multilayer process of 5/5 alumina/silica cycles apiece. We purposefully tried to fracture one of the shells (after the ALD run was complete) to obtain a better image of the surface vs. bulk composition. From Image B in Figure 11, it is clear that the majority of deposition occurred on the outer surface of the pyrolytic carbon shell but some of the ALD precursors were able to penetrate deeper into the shell for deposition.

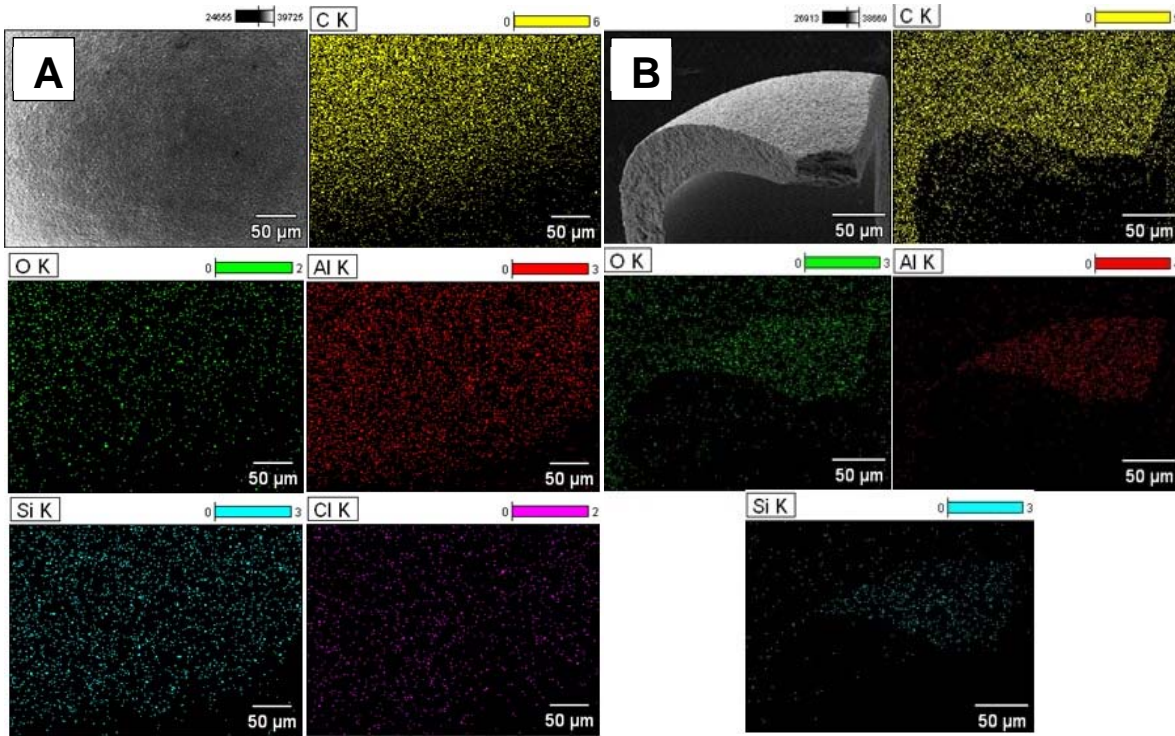


**Figure 11.** SEM and EDS mapping of **(A)** 20 multilayer coated  $5 \text{ Al}_2\text{O}_3 + 5 \text{ SiO}_2$  TRISO surrogate particles before and **(B)** 40 multilayer coated  $5 \text{ Al}_2\text{O}_3 + 5 \text{ SiO}_2$  surrogate particles after deposition conditions were modified to remove residual Cl atoms from  $\text{SiCl}_4$ , an ALD precursor for  $\text{SiO}_2$ .

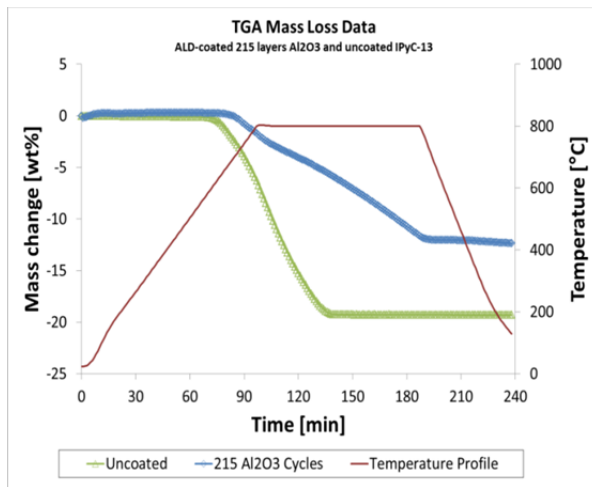


**Figure 12.** Temporal thermogravimetric data to show oxidation of the pyrolytic carbon shell of TRISO nuclear fuel surrogates in presence of air at  $800^\circ\text{C}$ .

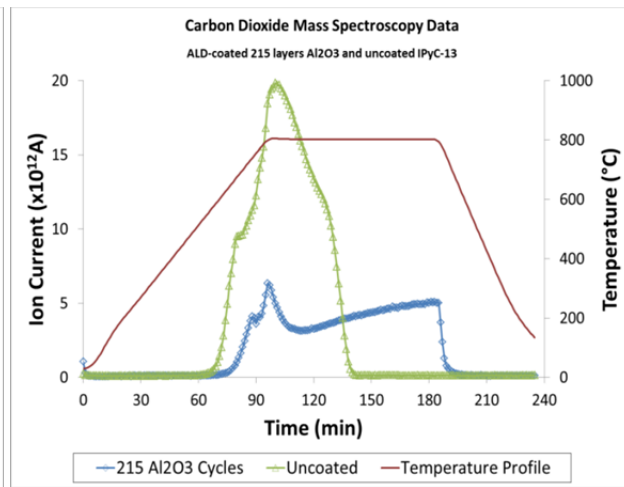


**Figure 13.** Mass spectrometry data showing evolution of  $\text{CO}_2$  as the CVD pyrolytic carbon shell oxidizes in the presence of dilute oxygen during the TGA run presented in Figure .

After demonstrating ALD was successful on TRISO surrogate fuel particles for varied ALD chemistries without surfactant treatment, thicker films were produced by high cycle numbers. ALD coatings can serve as effective oxygen barriers on carbon layers during elevated temperature exposure of air, as shown in Figure 12. TGA mass loss data for 215  $\text{Al}_2\text{O}_3$  ALD cycles deposited on TRISO surrogate particles using a fluidized bed reactor are compared to the mass loss data for uncoated TRISO particles. The temperature was ramped up to  $800^\circ\text{C}$  at a rate of  $8\text{K}/\text{min}$ , and held at that temperature

for 90 minutes. It is clear that the uncoated carbon shell began to lose mass at around 600°C, whereas the oxidation onset temperature for the coated carbon shell was around 700°C. This is an impressive result from the coefficient of thermal expansion mismatch perspective, as carbons are expected to expand much more drastically than ceramics at these high temperatures. The integrity of the ultrathin ALD film is seemingly more durable than its bulk counterpart.

It was also noteworthy that during the 90 minute dwell at 800°C, the rate of oxidation of the coated material retarded significantly. It was hypothesized that this change was based on oxygen diffusion through the ceramic oxide film and it was decided that non-oxide ceramic ALD films might eliminate the oxygen diffusion and further reduce oxidation of the underlying carbon shell. The use of carbides for passivation from high temperature oxygen was not considered because of the cyclic reoxidation and carburization at elevated temperatures would extract carbon from the TRISO particle eventually depleting the pyrolytic carbon shell the ALD film was intended to protect. The use of nitrides was deemed the most prudent alternative, as ceramic nitrides undergo carbothermal reduction less readily than ceramic oxides. Aluminum nitride films had been deposited at temperatures of 250°C with TMA and anhydrous ammonia as precursors years prior to this project. TMA and anhydrous ammonia are both inexpensive and readily available compounds at sufficient purity for ALD processes. Anhydrous ammonia was necessary because the presence of water would produce Al<sub>2</sub>O<sub>3</sub> defects in the AlN film.

In conjunction with TGA data, in situ mass spectrometry was used to ensure that the reduction in observed mass loss due to the ALD coatings corresponded with a reduction in CO<sub>2</sub> byproducts produced. The mass spec trace for CO<sub>2</sub> is shown in Figure 13, and clearly shows the reduction and hindrance of carbon oxidation conferred by the presence of the Al<sub>2</sub>O<sub>3</sub> ALD film.

**Table 4. Mass of atomic O and N in TRISO surrogate particles from LECO TC600 Oxygen/Nitrogen Analyzer.**

Sample Name	% Nitrogen	% Oxygen	Mass (g)
TRISO uncoated	0.000513	18.499	0.100190
100 AlN on TRISO	0.075758	18.323	0.098198
100 AlN post-TGA	0.017728	20.038	0.055072
215 Al <sub>2</sub> O <sub>3</sub> on TRISO	0.001017	18.278	0.101081
215 Al <sub>2</sub> O <sub>3</sub> post-TGA	0.001211	18.616	0.081205

Deposition of AlN was successful and was proven as a more effective oxidation barrier for the TRISO carbon shell. Figure 14 clearly shows that only 100 layers of AlN conferred more oxidation resistance to the pyrolytic carbon shell than did 215 layers of Al<sub>2</sub>O<sub>3</sub>. These data support the prediction that nitride films do not undergo carbothermal reduction as readily as oxide films. Also, the nitride films reduce oxygen migration

through the film. AlN ALD films provide 3.5% more oxidation resistance to underlying carbon layers for half as many cycles as Al<sub>2</sub>O<sub>3</sub> ALD films and with the use of inexpensive precursors TMA and ammonia.

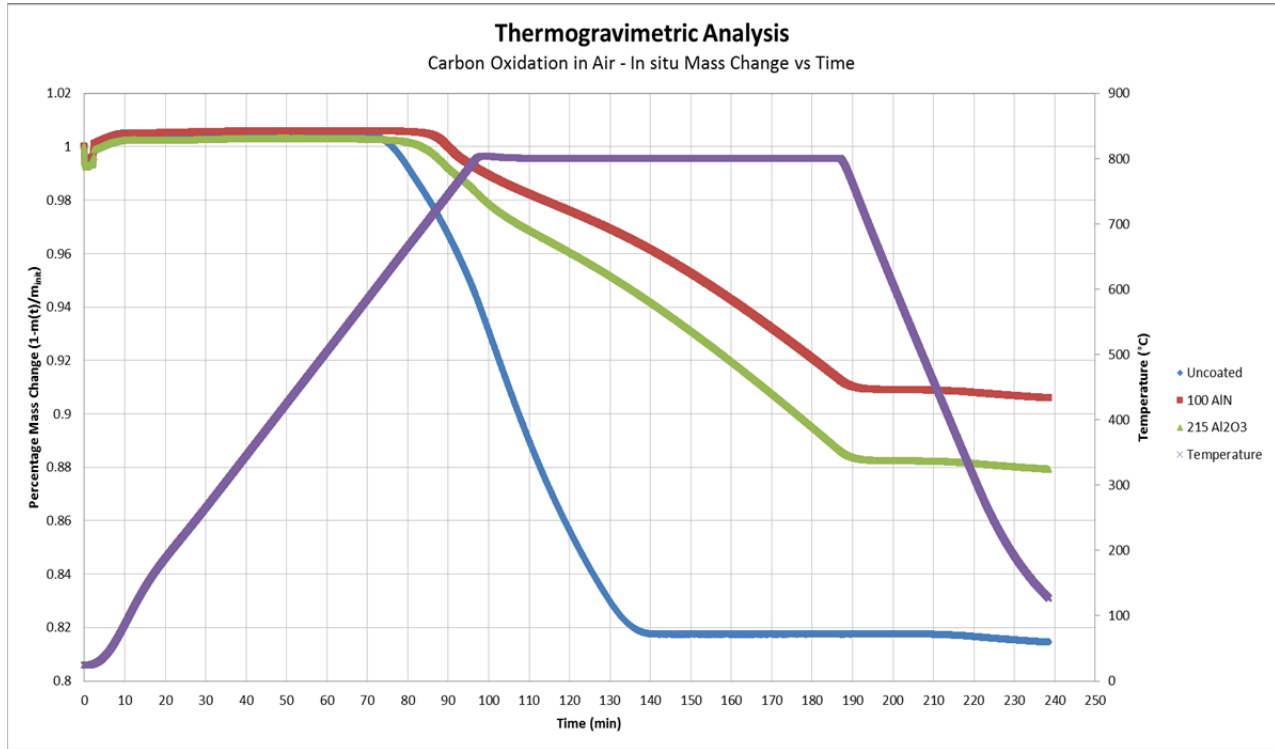


Figure 14. Temporal thermogravimetric data showing mass loss in dilute air up to 800C for 90 minutes. Plotted for comparison are (A) Uncoated TRISO, (B) 100 cycles AlN on TRISO, and (C) 215 cycles Al<sub>2</sub>O<sub>3</sub> on TRISO.

Efforts were made to positively confirm the presence of both Aluminum and Nitrogen in the film. Data obtained from analysis by LECO TC600 Oxygen/Nitrogen Analyzer in Table 4 clearly show the increased presence of Nitrogen in the TRISO surrogate particles coated with AlN. Inductively coupled plasma optical emission spectrum (ICP-OES) was utilized to confirm the presence of Aluminum, shown in Table 5. The amount of Aluminum reported in Table 5 accounts exclusively for the ALD film since the TRISO carbon shell and ZrO<sub>2</sub> core were unaffected by the NaOH treatment, whereas both Al<sub>2</sub>O<sub>3</sub> and AlN are soluble in the NaOH solutions used prior to analysis. ICP-OES results also confirm that near equal amounts of Aluminum atoms were deposited on to the carbon shell surface for Al<sub>2</sub>O<sub>3</sub> and AlN ALD processes.

Table 5. ICP-OES showing Aluminum atomic concentrations for uncoated and ALD coated TRISO surrogate particles.

Sample Name	Al ppm
TRISO Uncoated	DL*
100 AlN on TRISO	1310
215 Al <sub>2</sub> O <sub>3</sub> on TRISO	607
*Machine Detection Limit (DL) = 0.007ppm	



## Conclusions

### ***Specific Aim 1***

Al<sub>2</sub>O<sub>3</sub> ALD has been demonstrated to reduce grain-growth rate in sintered Gd<sub>2</sub>O<sub>3</sub> compacts. Grain size and uniformity are maintained for ALD coated whereas uncoated substrates show larger mean grain size and distribution. Furthermore, the apparent pore frequency in a sintered compact decreases with the presence of an Al<sub>2</sub>O<sub>3</sub> ALD film, thus the density is increased. Mechanical strength and durability, as measured by hardness and modulus of elasticity, do not have a clear correlation to ALD film thickness, or even the presence an ALD film.

### ***Specific Aim 2***

ALD films were successfully deposited on pyrolytic carbon shells around surrogate fuel ZrO<sub>2</sub> cores. These ALD films were demonstrated to provide significant oxidation resistance to the underlying carbon layers at temperatures of 800°C with dilute air, typical reactor conditions for NGNP fuel sources. Nitride films were shown to provide improved performance over oxide films as oxidation barriers with no increased cost due to reaction conditions or reactant materials (ALD precursors). Further investigation of ALD nitride chemistry could yield even higher performance oxidation barriers for the pyrolytic carbon shell of NGNP fuel sources.

**Patents:** None; an SBIR/STTR proposal is planned to be submitted by ALD NanoSolutions, Inc. in 2012 pending compelling success in this project.

**Publications / Presentations:** One manuscript expected to be submitted during 2013 pertaining to Specific Aim 2, namely the use of AlN films made via ALD as effective oxidation barriers, out-performing more layers of Al<sub>2</sub>O<sub>3</sub>.

## Final Report

**Project Title:** ALD Coatings on Gd<sub>2</sub>O<sub>3</sub> Burnable Poison Nanoparticles and Carbonaceous TRISO Coating Layers

**Covering Period:** October 1, 2009 to September 30, 2012

**Date of Report:** November 8, 2012

**Recipient:** University of Colorado  
3415 Colorado Avenue  
JSCBB Campus Box 596 UCB  
Boulder, CO 80309-0596

**Award Number:** Contract 00090607

**Project Number:** 09-312

**Principal Investigator:** Alan W. Weimer, Department of Chemical and Biological Engineering, University of Colorado, Boulder, CO 80303-0596;  
[alan.weimer@colorado.edu](mailto:alan.weimer@colorado.edu)

## **Project Objective**

The objective of this project was to demonstrate the feasibility of using atomic layer deposition (ALD) to apply ultrathin neutron-absorbing, corrosion-resistant layers consisting of ceramics, metals, or combinations thereof, on particles for enhanced NGNP fuel pellets. The manufactured composite particles will ideally be used to address materials issues with Generation IV nuclear power plants, using scaled-up powder coating techniques developed at the University of Colorado.

This project was divided into two specific aims, one to address the primary degradation mechanism of the fuel pellet core, and one to address the primary degradation mechanism of the protective shells of the fuel pellet. The success of either of these concepts will lead to significant advancement toward solving materials issues in NGNP fuel pellets.

## Background

The proposed project scope falls under two main specific aims: 1) fabrication and analysis of Gd-containing ceramics via gas-phase functionalization of  $Gd_2O_3$  powders with ceramic coatings; 2) coating and analysis of graphite/carbide powders with the chemically inert  $ZrO_2/Zr_3N_4$ -containing layers on outer surfaces and within pores for carbon-based fuel pellet shell strengthening. The activities contained within this project are designed to improve the lifetime of NGNP fuel pellets

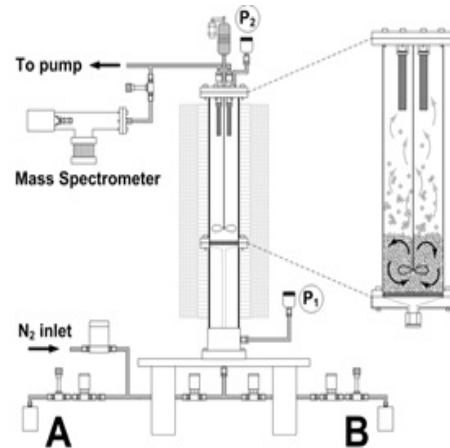


Figure 1. Schematic of ALD fluidized bed reactor.

Each of these specific aims can be achieved using the ALD technique, which has been used to deposit ceramic, metal and hybrid ceramic/polymer films on a variety of nano- and micron-sized particle (and other high surface area) substrates. Metal oxides and nitrides deposit in the form of conformal, pinhole-free films of nanoscale thickness, and metals tend to deposit as dispersed islands, resulting in nanoclusters of atoms. Experimental design techniques, either a factor analysis (full or fractional) or a central composite design (CCD) will be employed for the completion of each Milestone, as appropriate.

ALD is an analog of chemical vapor deposition (CVD) where reactive vapor precursors are administered to a reactor system individually, which chemically bonds one monolayer of the precursor (the “A” half-reaction) with all surface functional groups under saturating exposures. Upon completion, the first reactant is purged from the system, and the second one is then administered into the reactor, effectively eliminating an opportunity for gas-phase side-reactions. The second reaction, or “B” half-reaction, is allowed to proceed to completion before the B precursor is purged from the system. The sequential administration (or “dosing”) of each precursor can build a wide variety of ceramic films with angstrom-level precision. A schematic of the fluidized bed reactor used for Particle ALD is shown in Figure 1. ALD is an analog of CVD, but the two techniques are viable over two vastly different process windows. ALD is designed for ultrathin, precision-thickness films, whereas CVD is more ideal for building thick films where precision, conformity or porosity-free properties are not as critical. The process windows are shown in Figure 2.

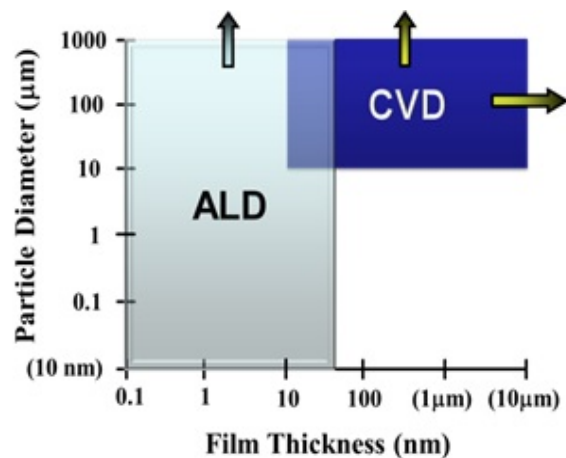


Figure 2. ALD and CVD process windows.

## Specific Aim 1 Outline

### *Improvements to the Fuel Pellet Core*

From a survey of recent literature, the composition and method of producing the NGNP fuel pellet kernel is a solid state reaction between primarily  $\text{UO}_2$  and  $\text{Gd}_2\text{O}_3$  powders. Current research efforts include evaluating additives, typically ceramics, which can be incorporated during the solid state reaction with the goal of improving the thermomechanical properties of the composite core. From a design perspective, the roles of the uranium-containing and gadolinium-containing components of the kernel are known as the source and moderator of neutron fluency, respectively.

The design goals of Specific Aim 1:

- a) **Improve structural integrity** of  $\text{Gd}_2\text{O}_3$  through incorporation of ceramic sub-phases without sacrificing too much gadolinium. The increasing content of a ceramic sub-phase is expected to increase structural integrity, while the decreasing content of the  $\text{Gd}_2\text{O}_3$  phase is expected to decrease neutron absorption. As such there is expected to be an optimal content ratio where value is added as measured by an improved fuel kernel lifetime.
- b) **Quantify thermal properties** of composite powders for modeling purposes. The predicted lifetime of the composite system should be modeled in order to optimize the content between the  $\text{Gd}_2\text{O}_3$  phase and the ceramic sub-phase. It is also thought that the energy required to form a mixed-metal oxide using solid state sintering techniques will be lower when using ALD-coated powders relative to the blending and sintering of primary oxide powders due to the lack of interdiffusion required for the former composition. An understanding of the energy requirements to manufacture the particles will help model the production cost at any scale.
- c) **Quantify crystal structure** and other physical properties of the produced ceramic composite powders. Both the content and crystal structure of the gadolinium oxide phase are important, as the thermomechanical properties of monoclinic  $\text{Gd}_2\text{O}_3$  has yielded a longer lifetime throughout its neutron absorption lifetime than the cubic phase. In addition, it is unknown precisely how the formation of mixed-metal oxides (e.g.  $\text{GdAlO}_3$ ,  $\text{Gd}_2\text{TiO}_4$ , etc.) will behave when derived using the atomic layer deposition process to produce the ceramic sub-phase. The grain size of a system typically has direct implications on its mechanical properties, with smaller grains leading to a decreased likelihood of crack propagation. Therefore the crystal structure, composition and grain size of each structure are important for predicting the expected gains in NGNP kernel technology using the ALD technique.
- d) **Quantify mechanical properties** of Gd-containing ceramic matrix composites, including thermal expansion. One failure mode for NGNP fuel pellets is the migration of the kernel in the direction of least resistance. Any anisotropy to

thermal flux and/or thermal expansion coefficients will increase the probability of catastrophic failure of the system. Sound methods should be devised and followed to demonstrate the tensile strength of the composite system.

## Specific Aim 1 Results

First, the cost of various  $Gd_2O_3$  sources were investigated as well as some of the particle characteristics that affect performance as an ALD substrate and neutron absorption material, such as BET Surface Area and crystal structure, respectively. The cost of micron-sized  $Gd_2O_3$  particles was found to be equivalent to the cost of gadolinium oxalate hydrate particles, on a per-Gd basis.  $Gd_2O_3$  nanopowder approaches four times the cost of other  $Gd_2O_3$  substrates. The surface area of  $Gd_2O_3$  derived through the decomposition of the gadolinium oxalate powder had eight times the surface area of the micron-sized  $Gd_2O_3$  powder. Incorporation of ceramic phases by ALD surface coatings is more efficient on a higher surface area powder (process time to achieve target weight percent) so gadolinium oxalate as the source material is favorable. Cryogenic milling of the gadolinium oxalate powder did not yield a dramatic increase in surface area (via particle size reduction), so the process intensity of the milling process is not worth the cost. Industrially produced  $Gd_2O_3$  nanopowder has the highest surface area but is unjustifiably expensive when compared to the performance of the  $Gd_2O_3$  powder derived from Gd-oxalate decomposition.

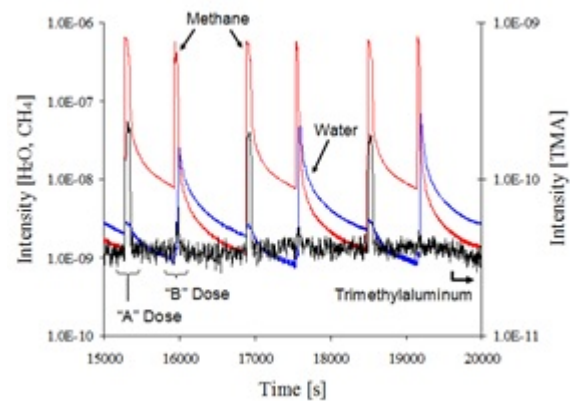


**Figure 3. Mass spectrometry data for three arbitrary consecutive  $Al_2O_3$  ALD cycles coated on  $Gd_2O_3$  particles. TMA, water, and their reaction product, methane, are shown.**

The incorporation of  $Al_2O_3$  phases onto  $Gd_2O_3$  powders using the ALD technique was successful. A typical mass spectrometry plot is shown in Figure 3, which tracks the evolution of methane throughout an  $Al_2O_3$  reaction process between trimethylaluminum (TMA) and water. TEM images were taken for the composite powders with the highest alumina contents, and are shown in Figure 4. The conformal, nano-scale films can be seen very clearly for all samples. The high quality results observed were of typical precision for Particle ALD.

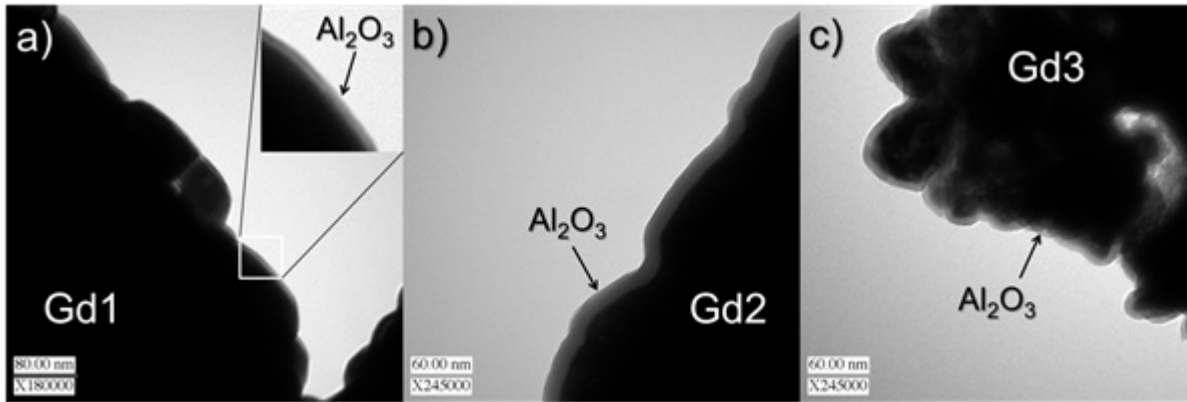


Figure 4. TEM images of Al<sub>2</sub>O<sub>3</sub> ALD films deposited on Gd<sub>2</sub>O<sub>3</sub> particles: (a) 100 cycles; (b) 60 cycles; (c) 40 cycle.

Attempts were also made to deposit films other than alumina, namely TiO<sub>2</sub> and Gd/Gd<sub>2</sub>O<sub>3</sub>. The difficulties associated with TiO<sub>2</sub> ALD proved to be insurmountable, and using the typical, inexpensive TiO<sub>2</sub> precursors, TiCl<sub>4</sub> and H<sub>2</sub>O, was detrimental to the particle substrate. TiO<sub>2</sub> via TiCl<sub>4</sub> converted the surface of the Gd<sub>2</sub>O<sub>3</sub> powder into GdCl<sub>3</sub>, which was highly undesirable so the task was abandoned. A Gd<sub>2</sub>O<sub>3</sub> ALD process was also attempted, and though the deposition reactions were successful, it was determined that the low growth rate and relatively high cost of the precursor made it an imprudent strategy, especially in light of the very positive results of the Al<sub>2</sub>O<sub>3</sub> ALD process on Gd<sub>2</sub>O<sub>3</sub> substrates.

Initially, compact fabrication techniques were developed to form stable pellets via cold pressing followed by sintering at atmospheric pressure. The thermal expansion of the uncoated Gd<sub>2</sub>O<sub>3</sub> blended with alumina nanopowder, as well as the alumina-coated gadolinia was measured using the dilatometer procured through a NEUP Infrastructure award. The thermal expansion of ALD-coated powders was found to be generally lower than the expansion of pellets that consist of blended powders. This is attributed to the homogeneous coating process, which guarantees that the alumina content is identical on both a macroscopic and microscopic level.

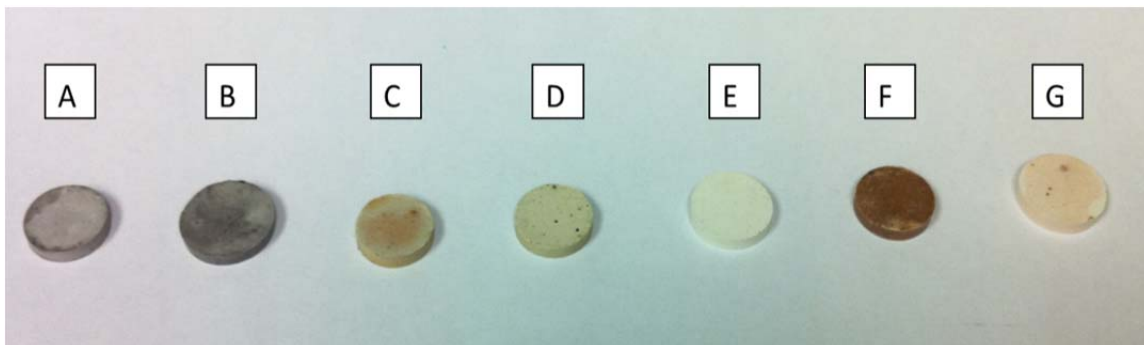


Figure 5. Photograph of coated and uncoated gadolinium (III) oxide pellets cold-pressed and sintered to 1450°C in air. (A) Gd<sub>2</sub>O<sub>3</sub> from Gd-Ox, (B) Gd<sub>2</sub>O<sub>3</sub> from Sigma Aldrich, (C) 9 Al<sub>2</sub>O<sub>3</sub> on Gd<sub>2</sub>O<sub>3</sub> from cryomilled Gd-Ox Decomp, (D) 20 Al<sub>2</sub>O<sub>3</sub> on Gd<sub>2</sub>O<sub>3</sub> from cryomilled Gd-Ox, (E) 12 Al<sub>2</sub>O<sub>3</sub> on Gd<sub>2</sub>O<sub>3</sub> from Gd-Ox Decomp, (F) 40 Al<sub>2</sub>O<sub>3</sub> on Gd<sub>2</sub>O<sub>3</sub> from Gd-Ox Decomp, (G) 60 Al<sub>2</sub>O<sub>3</sub> on Gd<sub>2</sub>O<sub>3</sub> from Gd-Ox Decomp.

The dilatometer results of these sintered pellets are presented in Figure 6. The temperature range 300°C – 1100°C was used to calculate the coefficient of linear thermal expansion,  $\alpha_L$ . The tests were run at 1 K/min from 25°C to 1500°C in an argon atmosphere. CTE values from Figure 6. Strain data from 300C to 1100C. The slope of

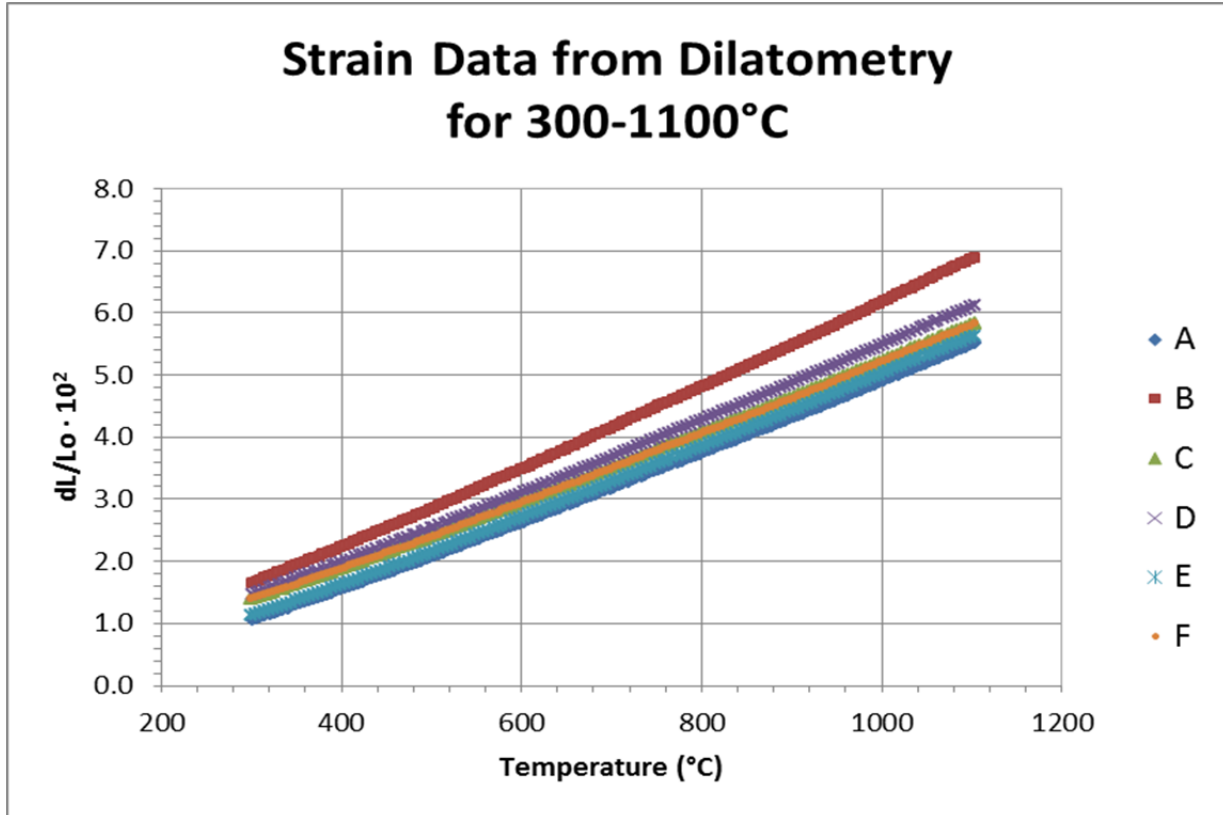


Figure 6. Strain data from 300C to 1100C. The slope of the line yields the coefficient of thermal expansion. (A) Uncoated Gd<sub>2</sub>O<sub>3</sub> from decomposed Gd-oxalate, (B) Uncoated Gd<sub>2</sub>O<sub>3</sub> from Sigma Aldrich, (C) 9 cycles ALD-Al<sub>2</sub>O<sub>3</sub> on Gd<sub>2</sub>O<sub>3</sub> from cryomilled-decomposed Gd-oxalate, (D) 20 cycles ALD-Al<sub>2</sub>O<sub>3</sub> Gd<sub>2</sub>O<sub>3</sub> from cryomilled-decomposed Gd-oxalate, (E) 12 cycles ALD-Al<sub>2</sub>O<sub>3</sub> on Gd<sub>2</sub>O<sub>3</sub> from decomposed Gd-oxalate, (F) 40 cycles ALD-Al<sub>2</sub>O<sub>3</sub> on Gd<sub>2</sub>O<sub>3</sub> from decomposed Gd-oxalate.

the line yields the coefficient of thermal expansion. (A) Uncoated Gd<sub>2</sub>O<sub>3</sub> from decomposed Gd-oxalate, (B) Uncoated Gd<sub>2</sub>O<sub>3</sub> from Sigma Aldrich, (C) 9 cycles ALD-Al<sub>2</sub>O<sub>3</sub> on Gd<sub>2</sub>O<sub>3</sub> from cryomilled-decomposed Gd-oxalate, (D) 20 cycles ALD-Al<sub>2</sub>O<sub>3</sub> Gd<sub>2</sub>O<sub>3</sub> from cryomilled-decomposed Gd-oxalate, (E) 12 cycles ALD-Al<sub>2</sub>O<sub>3</sub> on Gd<sub>2</sub>O<sub>3</sub> from decomposed Gd-oxalate, (F) 40 cycles ALD-Al<sub>2</sub>O<sub>3</sub> on Gd<sub>2</sub>O<sub>3</sub> from decomposed Gd-oxalate. are presented in Table 1.

Table 1. Calculated coefficients of linear thermal expansion for gadolinium (III) oxide sintered pellets.

	Uncoated Gd <sub>2</sub> O <sub>3</sub>		ALD-coated, Cryomilled Gd <sub>2</sub> O <sub>3</sub>		ALD-coated Gd <sub>2</sub> O <sub>3</sub> from decomp. Gd-ox	
	Gd <sub>2</sub> O <sub>3</sub> from Gd-ox	Sigma Aldrich Gd <sub>2</sub> O <sub>3</sub>	9 cyc. Al <sub>2</sub> O <sub>3</sub>	20 cyc. Al <sub>2</sub> O <sub>3</sub>	12 cyc. Al <sub>2</sub> O <sub>3</sub>	40 cyc. Al <sub>2</sub> O <sub>3</sub>

$\alpha_{L,300-1100C}$ [10 <sup>-6</sup> /K]	53.7	62.7	53.4	55.3	54.3	53.3
---	------	------	------	------	------	------

From the data shown in Table 1, there is no clear relationship between ALD film thickness and linear coefficient of thermal expansion though from literature, a negative correlation was expected. It is evident that Gd<sub>2</sub>O<sub>3</sub> derived from the decomposition of Gd-oxalate has a reduced thermal expansion compared to industrially manufactured 99.9% pure gadolinium oxide powder.

Using a HIP after cold-pressing pellets maintained the shape of the compacts and was a viable route to producing reliable substrates. For additional rigidity before putting pellets into the HIP, a sintering step at atmospheric pressure also appears to be beneficial, if transporting materials between pieces of equipment is an issue during manufacturing. Interestingly, there was a color change between the starting powder and the sintered compacts believed to result from complete decomposition of the Gd-oxalate into Gd<sub>2</sub>O<sub>3</sub>.

An important component of thermo mechanical testing of the ALD-coated Gd<sub>2</sub>O<sub>3</sub> material was nano-indentation analysis to determine modulus of elasticity and hardness. These pellets were prepared by first cold-pressure compaction, followed by hot isostatic pressing to 1450°C and 100 MPa, and finally by polishing the test surface to 3 microns.

**Table 2. Nano-indentation results for Gd<sub>2</sub>O<sub>3</sub> substrates, some of which were coated with Al<sub>2</sub>O<sub>3</sub>-ALD.**

Sample Name	Avg. Modulus (GPa)	Std. Dev.	Avg. Hardness (GPa)	Std. Dev.	Avg. Unload Modulus (GPa)	Std. Dev.	Avg. Unload Hardness (GPa)	Std. Dev.
Commercial Gd <sub>2</sub> O <sub>3</sub>	81.6	31.9	2.95	1.91	72.8	22.5	2.86	1.41
25 Al <sub>2</sub> O <sub>3</sub> on commercial Gd <sub>2</sub> O <sub>3</sub>	78.4	32.5	3.68	1.48	67.5	36.9	3.28	1.48
50 Al <sub>2</sub> O <sub>3</sub> on commercial Gd <sub>2</sub> O <sub>3</sub>	72.9	28.1	2.66	1.93	71.8	20.0	2.55	1.26
Gd <sub>2</sub> O <sub>3</sub> from cryomilled and decomposed Gd-oxalate	101	28.1	3.99	1.57	88.1	34.0	3.41	1.60
9 Al <sub>2</sub> O <sub>3</sub> on Gd <sub>2</sub> O <sub>3</sub> from cryomilled and decomposed Gd-oxalate	167	30.0	8.86	2.56	139	32.9	7.35	1.48
12 Al <sub>2</sub> O <sub>3</sub> on Gd <sub>2</sub> O <sub>3</sub> from cryomilled and decomposed Gd-oxalate	113	28.6	5.18	2.28	96.8	18.0	4.09	1.35
20 Al <sub>2</sub> O <sub>3</sub> on Gd <sub>2</sub> O <sub>3</sub> from decomposed Gd-oxalate	71.4	34.4	4.33	1.34	57.9	32.0	3.32	1.27

40 Al <sub>2</sub> O <sub>3</sub> on Gd <sub>2</sub> O <sub>3</sub> from decomposed Gd-oxalate	108	43.1	4.13	2.29	79.0	31.6	3.28	1.71
60 Al <sub>2</sub> O <sub>3</sub> on Gd <sub>2</sub> O <sub>3</sub> from decomposed Gd-oxalate	104	36.1	4.01	1.64	87.1	31.2	3.16	1.29

With respect to modulus of elasticity, there is a loose negative correlation to ALD film thickness. As the film thickness increases, the modulus of elasticity decreases, which is likely due the non-crystalline, amorphous structure of the ALD film. Unfortunately, no statistically significant assertion can be made with respect to ALD film thicknesses effect on elasticity and hardness due to the large standard deviation associated with each nano-indentation measurement presented in Table 2.

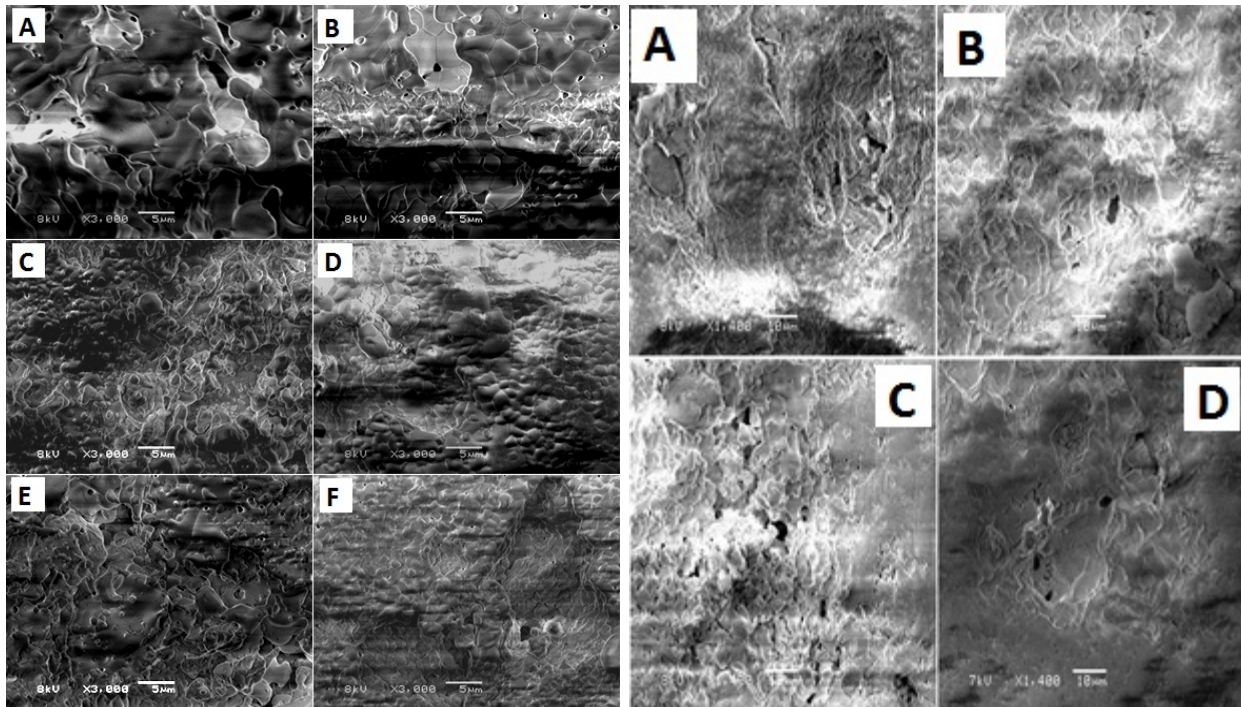


**Figure 7.** 3000X SEM images of sintered gadolinium oxide substrates. (A) Uncoated Gd<sub>2</sub>O<sub>3</sub> from Gd-ox, polished gadolinium oxide pellets. (B) Uncoated Sigma Aldrich Gd<sub>2</sub>O<sub>3</sub>, (C) 9 cycles Gd<sub>2</sub>O<sub>3</sub> from Sigma-Aldrich, (D) 20 cycles Al<sub>2</sub>O<sub>3</sub> on Gd<sub>2</sub>O<sub>3</sub> from Gd-ox, (E) 12 cycles Al<sub>2</sub>O<sub>3</sub> on cryomilled Gd<sub>2</sub>O<sub>3</sub> from Gd-ox, (F) 40 cycles Al<sub>2</sub>O<sub>3</sub> on Gd<sub>2</sub>O<sub>3</sub> from Gd-ox.

**Figure 8.** 1400X SEM images of sintered, HIPped, and uncoated surfaces. (A) Uncoated Sigma Aldrich Gd<sub>2</sub>O<sub>3</sub>, (B) 50 Al<sub>2</sub>O<sub>3</sub> on Gd<sub>2</sub>O<sub>3</sub> from Gd-ox, (C) Uncoated cryomilled Gd<sub>2</sub>O<sub>3</sub> from Gd-ox, (D) 12 Al<sub>2</sub>O<sub>3</sub> on cryomilled Gd<sub>2</sub>O<sub>3</sub> from Gd-ox.

The large standard deviations for each measurement (upwards of 50% of the mean value) were believed to be attributed to the amorphous structure of both the gadolinium substrates and the ALD films. Crystalline silica used to calibrate the nano-indentation instrument showed standard deviations of less than 5% for modulus of elasticity and hardness. High temperature and high pressure sintering performed in a hot isostatic press combined with surface polishing to 3 microns were intended to mitigate the large standard deviations but were unsuccessful. More reliable modulus of elasticity and hardness values could be obtained from crystalline composites, which might be achieved at temperatures approaching 1680°C.

Another important component of the thermochemical analysis of the  $Gd_2O_3$  material was SEM imagery to determine the grain size of the sintered gadolinia substrates. Figure 7 presents SEM images of sintered  $Gd_2O_3$  pellet surfaces and highlights the difference in grain size between coated and uncoated powders. Powders that were not coated with  $Al_2O_3$ -ALD show much larger grain size than those that were coated. Furthermore, powders coated with thicker  $Al_2O_3$  films showed smaller grain sizes after sintering than powders coated with thinner  $Al_2O_3$  films. Comparisons of similar substrates with either thin or thick coatings, C to E and D to F, respectively, show relationship between grain growth and ALD film thickness clear.

Figure 8 presents SEM photos obtained for fully dense pellets produced via cold-pressing followed by Hot Isostatic Pressing to 100 MPa and 1450°C that were polished to 3 microns on a diamond polishing wheel. It is evident from these images that the presence of  $Al_2O_3$  deposited via ALD simultaneously increases the uniformity of grain size and decreases the porosity, i.e. improves the sintering, for  $Gd_2O_3$ . ALD is demonstrated as a viable and effective method for increasing the final density of sintered substrates.

## Specific Aim 2

### *Improve the Lifetime of Carbonaceous TRISO Coating Layers*

The second specific aim was to coat nanometer-scale (or “nanothick”)  $ZrO_2$ , YSZ, BN/ $B_2O_3$  films on carbonaceous powders and test the high-temperature corrosion-resistance and thermo-mechanical properties of these chemically-inert ceramic materials. The CVD-derived, porous carbonaceous layers, namely C, PyC and SiC, are extremely sensitive to oxidation at high temperature, especially in low oxygen partial pressure environments found in nuclear reactors due to  $O_2$ , CO and  $H_2O$ . There is a desire to develop CVD techniques for ZrC as a method to provide enhanced corrosion-resistance to the fuel pellet layers. ALD techniques for  $ZrO_2$  and BN films have been demonstrated on particle surfaces, and YSZ and  $B_2O_3$  are simple extensions of proven technology. The ultimate goal is to deposit Zirconium-based coatings on carbonaceous substrates due to its low neutron absorption cross-section. Though BN may be very effective to create corrosion resistant carbons, it has the second highest neutron absorption cross section, making it a poor candidate for this aspect of the project. The precursor being used for Zr-based coatings is electronic grade tetrakis-(dimethylamido) Zirconium (TDMA-Zr), which is 99.99% pure. Hafnium absorbs neutrons at  $\sim 600x$  the rate of the equivalent amount of zirconium, and Hf is typically present in Zr compounds at 1-2%. The expense of this precursor is likely justified here, as the standard expense of removing Hf from Zr is alleviated through the purification of this compound.

Thus there was justification for this approach to providing corrosion-resistance properties to the porous CVD films due to the ability of ALD precursors to infiltrate pores and coat all exposed carbonaceous surfaces. Coated powders were tested using a high temperature thermogravimetric analyzer (HT-TGA) with dilute air environment in Argon.

The design goals of Specific Aim 2:

- a) **Develop ALD process methodologies to successfully coat carbons.** Carbonaceous materials are difficult to coat due to the lack of chemical functionality at the surfaces, and the ideal ALD technique relies on chemical bonding of molecular building blocks directly onto surfaces. There have been methods to physisorb molecules to the surfaces of carbons, and these and other molecules will be tested to obtain a pathway toward nano-functionalization.
- b) **Quantify high temperature oxidation resistance** of carbons after incorporation of ceramic sub-phases. Once the methodology has been developed,  $ZrO_2/Zr_3N_4$  and  $Y_2O_3/YN$  ALD processes can be developed and tested. It is thought that ceramic nitrides will have the greatest opportunity for success, as the presence of metal-nitrogen bonds tends to provide a much closer packed structure thus creating more effective diffusion barriers.
- c) **Quantify thermal cycling stability** of composite powders for modeling purposes. The thermal shock stability of ALD films will be a predictor of how well

the coatings will extend the lifetime of protective CVD layers on TRISO fuel pellets, and in turn provide a longer lasting nuclear fuel.

- d) **Identify potential fission byproduct scavenging materials.** This is an important goal that was not originally included in this proposal at the time it was written, and was added after attending the NEUP working meeting at ORNL in July 2010. Metals that can behave as either a cation or an anion have the greatest chance of being deposited by ALD (e.g. metal oxides or nitrides) and also be suitable for alloying to fission products and promote scavenging (e.g. silicides or aluminides). This is a strategy that deserves to be studied in Year 3 of this project, though may be difficult to validate experimentally without coating real, rather than surrogate, TRISO fuel pellets.

## Specific Aim 2 Results

As described in previous reports, coatings on carbons can be very difficult due to the inconsistent nature of surface functional groups. Methods to coat carbons must be developed case-to-case, as it is difficult to predict a carbonaceous substrate's functionality for ALD surface chemistry. Table 3 provides an overview of the historical progress made in the Weimer lab with using ALD to coat carbon particles, including work both within and outside the scope of this grant. The carbon substrate of most relevance to this project is the pyrolytic CVD carbon coated  $ZrO_2$  (TRISO surrogate) particles. Figure 9 shows TEM images along with corresponding EDS results of  $Al_2O_3$  and  $TiO_2$  ALD coatings successfully applied to carbon particles.

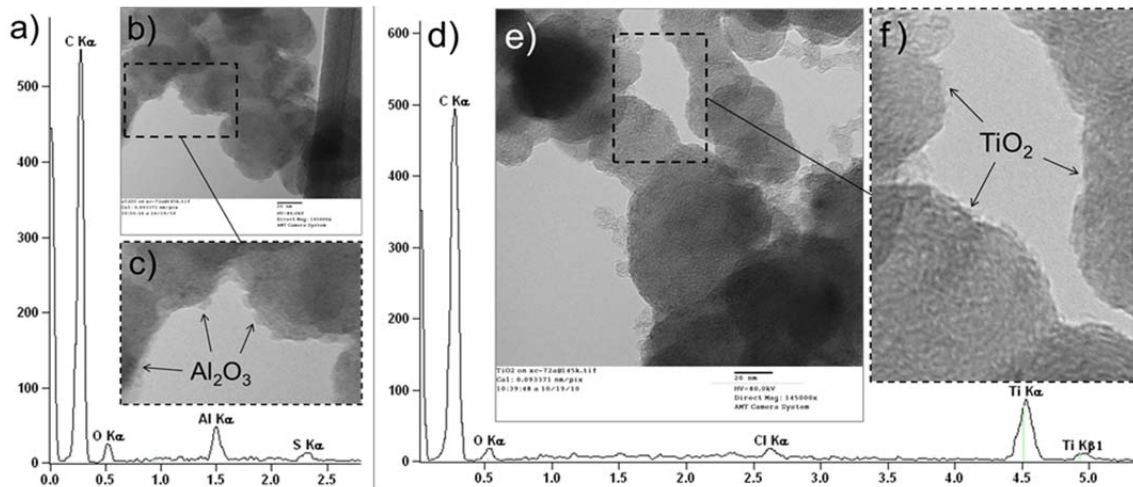


Figure 9. TEM images and EDS spectra of (a-c)  $Al_2O_3$  and (d-f)  $TiO_2$  on Cabot XC-72R carbon black.

Initially, the suitability of the TDMA-Zr precursor to  $ZrO_2$  ALD films for use in this project was determined by the following criteria: cost and ALD viability. Due to the low vapor pressure of TDMA-Zr at room temperature, heat was applied to the outer surface of the container to increase vapor pressure of the liquid inside. If future optimization is pursued, the center of the process window is 350°C. Though YSZ is a very good

candidate for a high strength coating material,  $ZrO_2$  has a very high thermal expansion coefficient, albeit decreasing with increasing  $Y_2O_3$  content. Therefore it may be beneficial to include  $Al_2O_3$ , or even high temperature metals such as Molybdenum or Tungsten, in multilayered fashion to the coating material of choice for cost reduction purposes while not sacrificing strength and oxidation resistance. The thermal expansion coefficients of many of the nitrides are about 50-60% of those of their oxides, and as such, the selection of each is transferrable across types of ceramics.

**Table 3. Description of relevant experience with performing ALD on carbonaceous substrates.**

Description	Coating Material(s)	Comments
Multi-walled carbon nanotubes	$Al_2O_3$	Conformal coating successful
Single-walled carbon nanotubes	$Al_2O_3$	Conformal coating unsuccessful; pre-treatment needed: $NO_2$ functionalization worked at small scale, liquid-phase pre-treatment (ethanol, surfactants) and drying prior to coating worked well
Diamond powder	$Al_2O_3$	Conformal coating successful
Graphite	$Al_2O_3$	Conformal coating unsuccessful; $NO_2$ functionalization did not work at larger scale
SPI Glassy Carbon	$Al_2O_3$	Conformal coating successful
Cabot XC-72R Vulcanized Carbon	$Al_2O_3$ , Alucone, $TiO_2$ , $B_2O_3$	Fuel Cell Grade Powder. Island growth successful, conformal coating limited by dispersion of sulfur sites from vulcanization process
TDA Research Carbon Black	$Al_2O_3$	Ultracapacitor Grade Powder. Difficult to coat, though surface area is $1900\text{ m}^2/\text{g}$ and may not be representative of difficult chemistry as much as non-ideal batch size
Pyrolytic CVD on surrogate TRISO	$Al_2O_3$ with surfactant pretreatment	Surfactant pretreatment process successfully led to ALD of alumina; 2Q11 focused on surfactant-free approaches

Initial laboratory efforts were focused around demonstration of ALD coatings on TRISO surrogate fuel pellets.  $Al_2O_3$  ALD from TMA and water by pre-treating the TRISO particles with sodium dodecylsulfate, a powerful surfactant was the first attempt. Figure 10 presents an SEM image of the coated TRISO particles with three locations where EDS mapping was performed: (1) the bulk surface, (2) within the bulk carbon layer of a cross-sectioned particle, and (3) the clearly white layer on the outer surface of the particle.

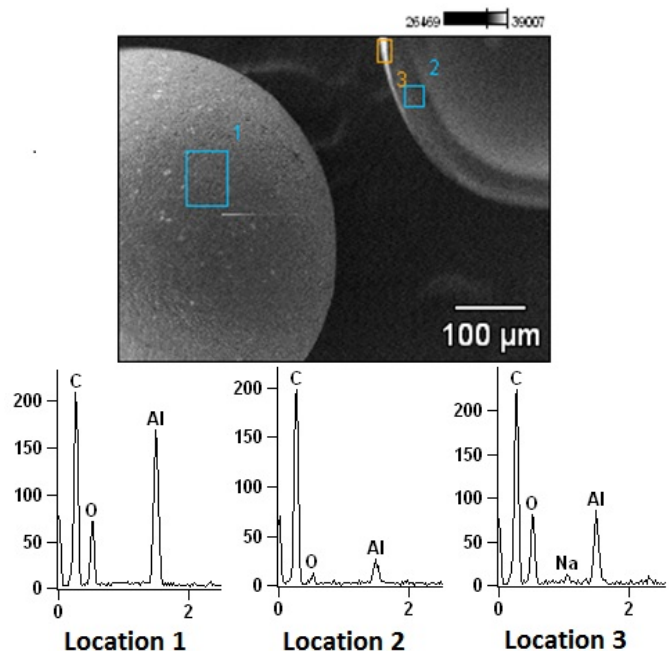


**Figure 10.** SEM and EDS mapping of TRISO surrogate fuel particles at three locations.

The surfactant pretreatment approach can be used to successfully deposit alumina on this type of carbon powder. As seen in the bulk surface spectrum (Location 1), the amount of surface aluminum is very close to the amount of carbon. The EDS spectrum of the carbon shell cross-section (Location 2) validates that the ALD process can infiltrate the porous CVD carbon network, though not as much as what can be coated on the external surface. This conclusion may be confounded by the liquid-phase surfactant pretreatment approach, as the liquid cannot penetrate through a porous layer as a gas-phase precursor can. From the cross-section of the outer edge of the carbon shell (Location 3) it is clear that some small amount of sodium remained on the TRISO pellet surface as a residual of the surfactant treatment. This is similar to what has been observed using this approach when coating single walled carbon nanotubes, and as such, was not surprising.

Subsequently, a surfactant-free ALD approach was developed for depositing  $\text{Al}_2\text{O}_3$  and  $\text{SiO}_2$  on to the pyrolytic carbon shell. Figure 11 Image A shows SEM and EDS mapping spectra from an ALD process where we carried out a multilayered ALD process, where 5  $\text{Al}_2\text{O}_3$  and 5  $\text{SiO}_2$  cycles were deposited per layer, and 20 multilayers were deposited. Evidence that both alumina and silica were present was confirmed, as well as the presence of residual chlorine from the  $\text{SiCl}_4$  precursor.

It was found that the presence of chlorine could be greatly reduced by altering key process conditions. The EDS mapping spectra below are from a 40 multilayer process of 5/5 alumina/silica cycles apiece. We purposefully tried to fracture one of the shells (after the ALD run was complete) to obtain a better image of the surface vs. bulk composition. From Image B in Figure 11, it is clear that the majority of deposition occurred on the outer surface of the pyrolytic carbon shell but some of the ALD precursors were able to penetrate deeper into the shell for deposition.

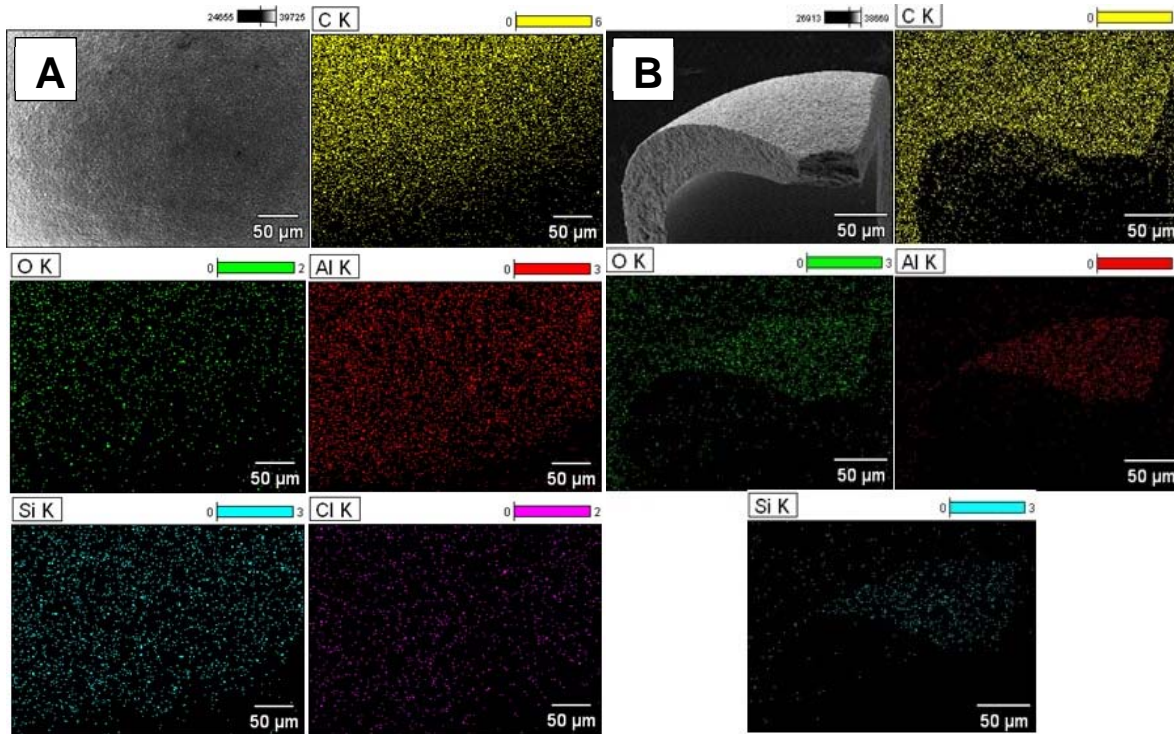


**Figure 11.** SEM and EDS mapping of **(A)** 20 multilayer coated  $5 \text{ Al}_2\text{O}_3 + 5 \text{ SiO}_2$  TRISO surrogate particles before and **(B)** 40 multilayer coated  $5 \text{ Al}_2\text{O}_3 + 5 \text{ SiO}_2$  surrogate particles after deposition conditions were modified to remove residual Cl atoms from  $\text{SiCl}_4$ , an ALD precursor for  $\text{SiO}_2$ .

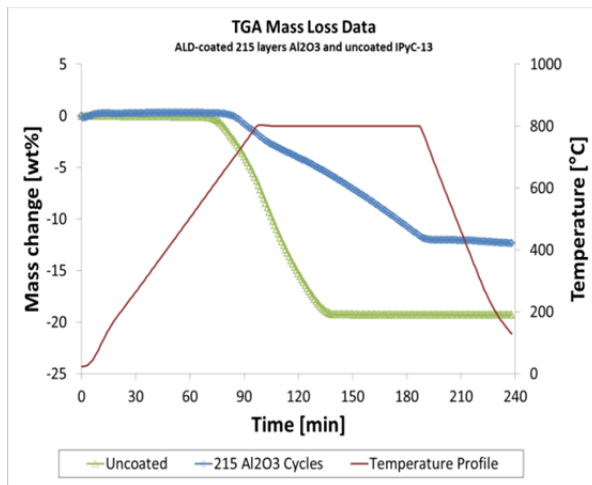


**Figure 12.** Temporal thermogravimetric data to show oxidation of the pyrolytic carbon shell of TRISO nuclear fuel surrogates in presence of air at  $800^\circ\text{C}$ .

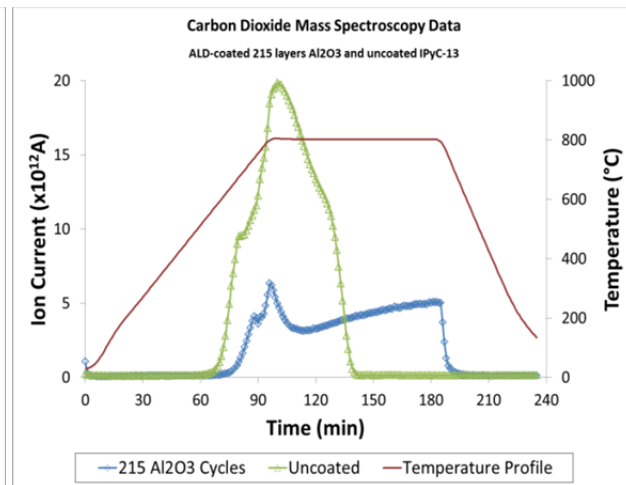


**Figure 13.** Mass spectrometry data showing evolution of  $\text{CO}_2$  as the CVD pyrolytic carbon shell oxidizes in the presence of dilute oxygen during the TGA run presented in Figure .

After demonstrating ALD was successful on TRISO surrogate fuel particles for varied ALD chemistries without surfactant treatment, thicker films were produced by high cycle numbers. ALD coatings can serve as effective oxygen barriers on carbon layers during elevated temperature exposure of air, as shown in Figure 12. TGA mass loss data for 215  $\text{Al}_2\text{O}_3$  ALD cycles deposited on TRISO surrogate particles using a fluidized bed reactor are compared to the mass loss data for uncoated TRISO particles. The temperature was ramped up to  $800^\circ\text{C}$  at a rate of  $8\text{K}/\text{min}$ , and held at that temperature

for 90 minutes. It is clear that the uncoated carbon shell began to lose mass at around 600°C, whereas the oxidation onset temperature for the coated carbon shell was around 700°C. This is an impressive result from the coefficient of thermal expansion mismatch perspective, as carbons are expected to expand much more drastically than ceramics at these high temperatures. The integrity of the ultrathin ALD film is seemingly more durable than its bulk counterpart.

It was also noteworthy that during the 90 minute dwell at 800°C, the rate of oxidation of the coated material retarded significantly. It was hypothesized that this change was based on oxygen diffusion through the ceramic oxide film and it was decided that non-oxide ceramic ALD films might eliminate the oxygen diffusion and further reduce oxidation of the underlying carbon shell. The use of carbides for passivation from high temperature oxygen was not considered because of the cyclic reoxidation and carburization at elevated temperatures would extract carbon from the TRISO particle eventually depleting the pyrolytic carbon shell the ALD film was intended to protect. The use of nitrides was deemed the most prudent alternative, as ceramic nitrides undergo carbothermal reduction less readily than ceramic oxides. Aluminum nitride films had been deposited at temperatures of 250°C with TMA and anhydrous ammonia as precursors years prior to this project. TMA and anhydrous ammonia are both inexpensive and readily available compounds at sufficient purity for ALD processes. Anhydrous ammonia was necessary because the presence of water would produce Al<sub>2</sub>O<sub>3</sub> defects in the AlN film.

In conjunction with TGA data, in situ mass spectrometry was used to ensure that the reduction in observed mass loss due to the ALD coatings corresponded with a reduction in CO<sub>2</sub> byproducts produced. The mass spec trace for CO<sub>2</sub> is shown in Figure 13, and clearly shows the reduction and hindrance of carbon oxidation conferred by the presence of the Al<sub>2</sub>O<sub>3</sub> ALD film.

**Table 4. Mass of atomic O and N in TRISO surrogate particles from LECO TC600 Oxygen/Nitrogen Analyzer.**

Sample Name	% Nitrogen	% Oxygen	Mass (g)
TRISO uncoated	0.000513	18.499	0.100190
100 AlN on TRISO	0.075758	18.323	0.098198
100 AlN post-TGA	0.017728	20.038	0.055072
215 Al <sub>2</sub> O <sub>3</sub> on TRISO	0.001017	18.278	0.101081
215 Al <sub>2</sub> O <sub>3</sub> post-TGA	0.001211	18.616	0.081205

Deposition of AlN was successful and was proven as a more effective oxidation barrier for the TRISO carbon shell. Figure 14 clearly shows that only 100 layers of AlN conferred more oxidation resistance to the pyrolytic carbon shell than did 215 layers of Al<sub>2</sub>O<sub>3</sub>. These data support the prediction that nitride films do not undergo carbothermal reduction as readily as oxide films. Also, the nitride films reduce oxygen migration

through the film. AlN ALD films provide 3.5% more oxidation resistance to underlying carbon layers for half as many cycles as Al<sub>2</sub>O<sub>3</sub> ALD films and with the use of inexpensive precursors TMA and ammonia.

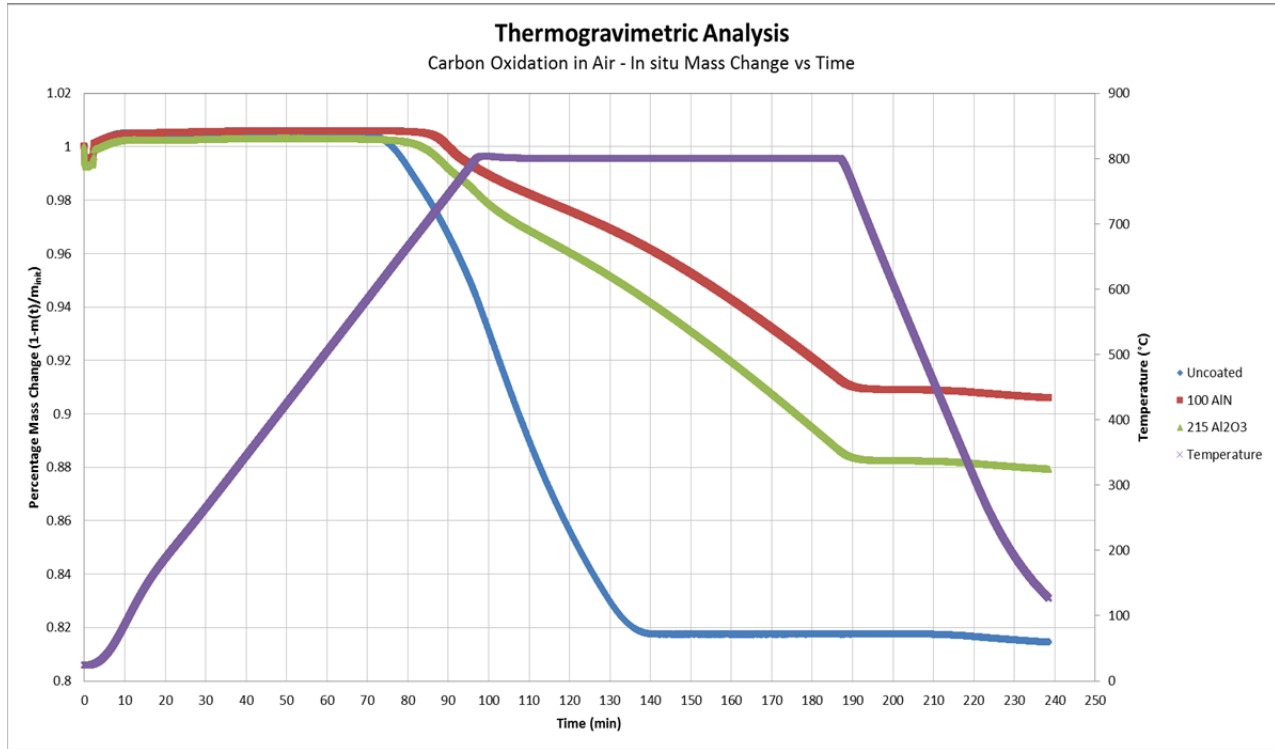


Figure 14. Temporal thermogravimetric data showing mass loss in dilute air up to 800C for 90 minutes. Plotted for comparison are (A) Uncoated TRISO, (B) 100 cycles AlN on TRISO, and (C) 215 cycles Al<sub>2</sub>O<sub>3</sub> on TRISO.

Efforts were made to positively confirm the presence of both Aluminum and Nitrogen in the film. Data obtained from analysis by LECO TC600 Oxygen/Nitrogen Analyzer in Table 4 clearly show the increased presence of Nitrogen in the TRISO surrogate particles coated with AlN. Inductively coupled plasma optical emission spectrum (ICP-OES) was utilized to confirm the presence of Aluminum, shown in Table 5. The amount of Aluminum reported in Table 5 accounts exclusively for the ALD film since the TRISO carbon shell and ZrO<sub>2</sub> core were unaffected by the NaOH treatment, whereas both Al<sub>2</sub>O<sub>3</sub> and AlN are soluble in the NaOH solutions used prior to analysis. ICP-OES results also confirm that near equal amounts of Aluminum atoms were deposited on to the carbon shell surface for Al<sub>2</sub>O<sub>3</sub> and AlN ALD processes.

Table 5. ICP-OES showing Aluminum atomic concentrations for uncoated and ALD coated TRISO surrogate particles.

Sample Name	Al ppm
TRISO Uncoated	DL*
100 AlN on TRISO	1310
215 Al <sub>2</sub> O <sub>3</sub> on TRISO	607
*Machine Detection Limit (DL) = 0.007ppm	



## Conclusions

### ***Specific Aim 1***

Al<sub>2</sub>O<sub>3</sub> ALD has been demonstrated to reduce grain-growth rate in sintered Gd<sub>2</sub>O<sub>3</sub> compacts. Grain size and uniformity are maintained for ALD coated whereas uncoated substrates show larger mean grain size and distribution. Furthermore, the apparent pore frequency in a sintered compact decreases with the presence of an Al<sub>2</sub>O<sub>3</sub> ALD film, thus the density is increased. Mechanical strength and durability, as measured by hardness and modulus of elasticity, do not have a clear correlation to ALD film thickness, or even the presence an ALD film.

### ***Specific Aim 2***

ALD films were successfully deposited on pyrolytic carbon shells around surrogate fuel ZrO<sub>2</sub> cores. These ALD films were demonstrated to provide significant oxidation resistance to the underlying carbon layers at temperatures of 800°C with dilute air, typical reactor conditions for NGNP fuel sources. Nitride films were shown to provide improved performance over oxide films as oxidation barriers with no increased cost due to reaction conditions or reactant materials (ALD precursors). Further investigation of ALD nitride chemistry could yield even higher performance oxidation barriers for the pyrolytic carbon shell of NGNP fuel sources.

**Patents:** None; an SBIR/STTR proposal is planned to be submitted by ALD NanoSolutions, Inc. in 2012 pending compelling success in this project.

**Publications / Presentations:** One manuscript expected to be submitted during 2013 pertaining to Specific Aim 2, namely the use of AlN films made via ALD as effective oxidation barriers, out-performing more layers of Al<sub>2</sub>O<sub>3</sub>.